

Degradation of signals and operation failures of radio engineering satellite systems during geospace disturbances accompanied by abrupt changes in the geomagnetic field

E. L. Afraimovich

Institute of Solar-Terrestrial Physics SD RAS,
p. o. box 4026, Irkutsk, 664033, Russia,
e-mail: afra@iszf.irk.ru

Abstract

During strong magnetic storms, the errors of determination of the range, frequency Doppler shift and angles of arrival of transitionospheric radio signals exceeds the one for magnetically quiet days by one order of magnitude as a minimum. This can be the cause of performance degradation of current satellite radio engineering navigation, communication and radar systems as well as of superlong-baseline radio interferometry systems. The relative density of phase slips at mid-latitudes exceeds its mean value for magnetically quiet days at least by the order of 1 or 2, that makes a few percent of the total density of GPS observations. Furthermore, the level of phase slips for the GPS satellites located at the sunward side of the Earth was 5-10 times larger compared to the opposite side of the Earth.

1 Introduction

With the development of progress, our civilization is becoming increasingly dependent on technological navigation and radar systems whose performance is to a certain extent governed by geospace conditions. In an effort to pave the way for tackling the issues of vulnerability of technological systems, the US National "Space Weather" program was developed (<http://www.ofcm.gov/nswp-ip/text/cover.htm>).

Radio engineering satellite systems (RESS), with their ground-based and space-borne support facilities, are finding ever-widening application in various spheres of human activity. They are able to provide global coverage, accuracy, continuity, high reliability and meet a number of other requirements imposed when tackling a broad spectrum of engineering problems. However, the use of RESS also implies new (and, in some cases, more stringent) requirements dictated by the need to ensure safety and economical efficiency of the operation of ground-based and airborne facilities, as well as to solve special problems (observation, aerophotography, searching and rescue of distressed transport vehicles and people). This applies equally for performance of Global Navigation Satellite Systems (GNSS) as well as for very-long-baseline radio interferometers (VLBI) (Thompson et al., 1986).

Degradation of transitionospheric radio signals and operation failures during geospace disturbances constitute a crucial factor of space weather influence on SRNS performance (along with other factors such as spacecraft surface charging, nonuniform satellite drag, breakdowns of satellite electronics by high-energy particles, etc.).

One of the most dramatic examples of the RESS - GPS (Hofmann-Wellenhof et al., 1992) that has embodied many modern achievements at the interface of many sciences and technologies, has currently become a powerful factor of worldwide scientific and technical progress and is widely used in quite various realms of human activity. In this connection, much attention is given to continuous perfection of the GPS system and to the widening of the scope of its application for solving the navigation problems themselves, as well as for developing higher-precision systems for time and accuracy determinations. Even greater capabilities are expected in the near future through the combined use of the GPS with a similar Russian system GLONASS (Kharisov et al., 1998).

The broad prospects afforded by the use of positioning systems through the use of the SRNS dictate the need for a detailed study of the parameters of the satellite naviga-

tion systems themselves, including the reliability of their operation and noise immunity, especially when operated in extreme conditions (for instance, during large geomagnetic disturbances). To carry out such investigations requires considerable hardware, software and financial expenses incurred by the setting up of the necessary testing grounds for large sets of GPS-GLONASS receivers of different types, and for the development of dedicated software-hardware capabilities and facilities for data processing.

Meanwhile a global network of two-frequency multichannel GPS receivers is currently in operation, the data from which with a temporal resolution of 30 s are posted in a centralized fashion on the SOPAC server (<ftp://lox.ucsd.edu>) in a standard RINEX format (Gurtner, 1993) and made available for analysis and usage on the Internet. This network is being constantly expanded, and by January 2002 it consisted of more than 1000 registered GPS receivers, and the SOPAC server contain data of round-the-clock measurements from the receivers spanning a period of more than five years. The database, obtained in this way, represents unique material.

Using two-frequency multichannel receivers of the global navigation GPS system, at almost any point on the globe and at any time simultaneously at two coherently-coupled frequencies $f_1 = 1575.42$ MHz and $f_2 = 1227.60$ MHz, highly accurate measurements of the group and phase delays are being underway along the line of sight (LOS) between the receiver on the ground and the transmitters on-board the GPS system satellites which are in the zone of reception.

These data, converted to values of total electron content (TEC), are of considerable current use in the study of the regular ionosphere and of disturbances of natural and technogenic origins (solar eclipses, flares, earthquakes, volcanoes, strong thunderstorms, auroral heating, nuclear explosions, chemical explosion events, launches of rockets). We do not cite here the relevant references for reasons of space, which account for hundreds of publications to date.

These prospects make the use of the global GPS network attractive for the implementation of the above-mentioned research, for preliminary accumulation of the sample statistic, as well as for carrying out analyses and modelings with the purpose of studying the GPS-GLONASS. All this would make it possible to optimize the expenditures incurred by the creation of research grounds and by tests, as well as to obtain preliminary results virtually without any expenses for acquisition of equipment.

Of special interest from the scientific and practical standpoint within the "Space

“Weather” program is the development of a new (based on the latest achievements) geospace monitoring technology and the analysis of the whole set of ionospheric disturbances of natural and technogenic origin.

The ideology and automated software complex GLOBDET for global GPS detection and monitoring of ionospheric disturbances has been developed at the ISTP SB RAS. GLOBDET makes it possible to automate the acquisition, filtering and pretreatment process of the GPS data received via the Internet (Afraimovich, 2000a).

This technology is being used to detect, on a global and regional scales, ionospheric effects of strong magnetic storms (Afraimovich et al., 1998b; 2002e), solar flares (Afraimovich, 2000a; Afraimovich et al., 2001f), solar eclipses (Afraimovich et al., 2002d), launches of rockets (Afraimovich et al., 2001e), earthquakes (Afraimovich et al., 2001g), etc.

The global GPS detector distinguishes from previously available ionospheric radio sounding facilities by the continuity of observations, high spatial and temporal resolution and high sensitivity, as well as by standardization and adaptability of data processing. The global GPS detector can also be used as a tester of the transitionospheric radio channel of propagation of signals from space-based radio-engineering systems and space radio sources.

The objective of this paper is to demonstrate - on the basis of using the GLOBDET technology - how ionospheric disturbances during magnetic storms contribute to the degradation of signals and failures of the GPS system.

2 General information about the database used

This study relies on the data from the global network of receiving GPS stations available on the Internet (Fig.1). As is evident from Fig.1, the receiving sites are relatively dense on the territory of North America and Europe, and less as dense in Asia. Fewer stations are located on the Pacific and Atlantic.

Such coverage of the terrestrial surface by GPS receivers makes it possible, already at the present time, to address the problem of a global investigation of ionospheric disturbances and their consequences with a very large spatial accumulation.

Thus, in the Western hemisphere the corresponding number of stations is as large as 500, and the number of LOS's to the satellite is at least 2000...3000. This provides a number of statistically independent series at least two orders of magnitude higher than would be realized by recording VHF radio signals from first-generation geostationary satellites or low-orbit navigation satellites - TRANSIT (Gershman et al., 1984).

This study is based on using the data from a global network of GPS receiving stations available from the Internet (<http://lox.ucsd.edu>). For a number of reasons, slightly differing sets of GPS stations were chosen for the various events under investigation; however, the experimental geometry for all events was virtually identical. The analysis used a set of stations (from 160 to 323) with a relatively even distribution across the globe. For reasons of space, we do not give here the stations coordinates. This information may be obtained from <http://lox.ucsd.edu/cgi-bin/allCoords.cgi?>.

The analysis involved four days of the period 1999-2000, with the values of the geomagnetic field disturbance index Dst ranging from 0 to -295 nT and Kp from 3 to 9. The maximum values of the geomagnetic field disturbance index Dst_{max} and Kp_{max} are listed in Table 1.

The statistic of the data used in this paper for mid-latitudes and for each of the days under examination is characterized by the information in Table 1 about the number of stations used m and number of LOS's n .

3 Influence of the ionosphere on transitionospheric radio signal characteristics

The performance of modern global satellite radio navigation systems that utilize the "Earth-Space" radio wave propagation channel is limited considerably by the influence of the geospace environment. Furthermore, the main contribution comes from systematic ionospheric effects of radio wave propagation: the group and phase delay, the frequency Doppler shift, and the rotation of the plane of polarization (Faraday effect). In many instances the degree of manifestation of the above effects has only a weak dependence on the local distribution of electronic density in the ionosphere but is directly correlated with the value of total electron content (TEC) along the radio signal propagation path (Goodman and Aarons, 1990).

In undisturbed geospace conditions the main contribution to the formation of the above-mentioned ionospheric effects is made by the regular TEC component. It undergoes periodic regular variations (seasonal-diurnal, latitudinal, and longitudinal) and is relatively accurately predictable. A variety of TEC models have been developed to date, which are intended to cancel out the ionospheric influence on the performance of the modern GLONASS and GPS in geomagnetically quiet and weakly disturbed conditions (Afraimovich et al., 2000b; Klobuchar, 1986).

The situation with geomagnetically disturbed geospace is more complicated. The irregular TEC component makes a substantial contribution in this case. The amplitude of random TEC variations with a period from a few minutes to several hours in conditions of geomagnetic disturbances can make up as much as 50% of the background TEC value (Basu et al., 1988; Bhattacharrya et al., 2000; Ho et al., 1996; Shaer et al., 1997; Warnart, 1995). Furthermore, the amplitude and phase fluctuation range of signals from navigation satellites (NS) at the reception point can exceed the designed level corresponding to the uninterrupted operation of GPS receivers.

This leads to the degradation of the determination accuracy of a current location of stationary and mobile users of GPS. Furthermore, there might occur a break-down in tracking the NS signal in phase (code) one of the working frequencies and, hence, a failure in the determination of the coordinates in the one- or two-frequency mode (Scone and Jong, 2000; 2001; Coster et al., 2001; Afraimovich et al., 2002c).

The key characteristic of the ionosphere that determines the variation of radio wave

parameters is the integral (total) electron content (TEC) $I(t)$ or its derivatives (with respect to time and space) I'_t , I'_x and I'_y along the propagation path (Davies, 1969; Kolosov et al., 1969; Yakovlev, 1985; Goodman and Aarons, 1990; Afraimovich et al., 1992; Yakubov, 1997).

TEC variations may be arbitrarily classified as regular and irregular. Regular changes (seasonal, diurnal) - for the magnetically quiet mid-latitude ionosphere at least - are described by models providing relative accuracy of TEC prediction in the range 50...80%. Irregular changes (variations) are associated with ionospheric irregularities of a different nature, the spectrum of which has a power law character (Gajlit et al., 1983; Gershman et al., 1984; Yakubov, 1997).

TEC variations introduce proportionate changes of the signal phase $\varphi(t, x, y) = k_1 I(t, x, y)$, which gives rise to measuring errors of the range $\sigma D = k_2 dI$, the frequency Doppler shift of the signal $\sigma f = k_3 I'_t$, and the angles of arrival of the radio wave $\sigma \alpha_x = k_4 I'_x$ and $\sigma \alpha_y = k_4 I'_y$, because the last four quantities are proportional to the time and space derivatives of the phase. Furthermore, the maximum value of the measuring error of angular deviations can be deduced using the relation $\sigma \alpha = k_4 \sqrt{(I'_x)^2 + (I'_y)^2}$.

The coefficients $k_1 - k_4$ are inversely proportional to the signal frequency f_c or to its square (Davies, 1969; Kravtsov et al., 1983; Goodman and Aarons, 1990). A calculation uses a Cartesian topocentric coordinate system with the axis x pointing eastward E , and the axis y pointing northward N .

Investigations of phase fluctuations of transionospheric signals have been and are carried out using radio beacons on satellites with circular and geostationary orbits (Komrakov and Skrebkova, 1980; Livingston et al., 1981; Gajlit et al., 1983). The trouble with these measurements is that temporal and spatial resolution is low, and continuity and global coverage of observations are unavailable.

The use of the international ground-based network of two-frequency receivers of the GPS opens up new avenues for a global, continuous, fully computerized monitoring of phase fluctuations of signals and associated errors of RESS performance.

Some research results on the prediction and estimation of radio signal fluctuations and errors of RESS performance caused by them were reported in earlier work (Afraimovich and Karachenschev, 2002b).

Below we give an outline of the techniques used in this study and illustrate their application in the analysis of ionospheric effects. The overall sample statistic of errors

σD , σf and $\sigma \alpha$ is presented for different geomagnetic conditions. To ease comparison with other research results reported in (Gajlit et al., 1983; Kravtsov et al., 1983), the errors σD , σf and $\sigma \alpha$ are calculated for the working frequency of 300 MHz.

4 Analysis of the measuring errors of the range, Doppler frequency and angles of arrival of the radio wave caused by changes in the regular ionosphere

Recently a number of authors (Wilson et al., 1995; Mannucci et al., 1998; Schaer et al., 1998; and others) have developed a new technology for constructing Global Ionospheric Maps (GIM) of TEC using IONEX data from the international IGS-GPS network. The GIM technology and its uses have been reported in a large number of publications (Wilson et al., 1995; Mannucci et al., 1998).

The standard IONEX format is described in detail in (Schaer et al., 1998). Therefore, we will not give a detailed description of the GIM technology for reasons of space but limit ourselves only to the information required for the presentation of our method. Two-hour TEC maps are easily accessible to any user, which are calculated by several research groups in the USA and Europe and are available on the Internet in the standard IONEX format (<ftp://cddisa.gsfc.nasa.gov/pub/gps/products/ionex>). It is also possible to obtain 15-min maps if necessary.

Fig.2 is a schematic representation of a single elementary GIM cell. The cell nodes are designated as a , b , c , d . The cell size (5° in longitude and 2.5° in latitude) is determined by the IONEX file standard. For simplifying the transformations to an approximation sufficient for our problem for latitudes not exceeding 60° , the cell can be represented as a rectangle with the sides d_e and d_n . It is easy to overcome this limitation by complicating to a certain extent the transformations allowing for the sphericity; however, we do not present them in this report.

The linear size of the rectangular cell in latitude is independent of the latitude and is $d_e = 279$ km; the linear size in longitude depends on the latitude, and for $40^\circ N$ it is $d_n = 436$ km.

For each time t , for the nodes a , b , c , d from the IONEX file the values of vertical

TEC are known - I_a, I_b, I_c, I_d .

The determination of the range D by the phase method is based on measuring the phase difference φ between the received signal and the reference signal formed in the receiver. Such a measurement can be made at the intermediate or carrier frequency of the signal. In this case:

$$D = c \times \frac{\varphi}{2 \pi f_c} \quad (1)$$

where c is the propagation velocity of radio waves in a free space.

Generally the quantity φ for the transitionospheric propagation may be regarded as the sum of two components (Afraimovich et al., 1998a):

$$\varphi = \varphi_s + \Delta\varphi \quad (2)$$

where φ_s is the main component associated with a change of the distance between the signal source and the receiver.

Analysis of the measuring errors of the range, Doppler frequency and angles of arrival of the radio wave caused by changes in the regular ionosphere investigations of global phase variations of radio signals and their influence on the operation of RESS ought to take into account the proportionate relationship between phase (phase derivative) changes of the transitionospheric signal and corresponding TEC variations (Kravtsov et al., 1983; Goodman and Aarons, 1990):

$$\Delta\varphi = 8.44 \times 10^{-7} \times \frac{I_{a(b,c,d)}}{f_c} + \varphi_0 \quad (3)$$

where f_c is the radio wave frequency (Hz); $I_{a(b,c,d)}$ is the TEC measured at the points a, b, c , and d (10^{16} el/m^2); and φ_0 is the initial phase (Spoelstra and Kelder, 1984).

By way of example we now analyze the errors of measurement of the range σD , the frequency Doppler shift σf and the angle of arrival of the radio wave $\sigma\alpha$ using the IONEX data and the method that was developed at the ISTP SB RAS (Afraimovich and Karachenschev, 2002b).

The change of the range that is introduced by the ionosphere (ionospheric error) is proportional to $\Delta\varphi$:

$$\sigma D = c \times \frac{\Delta\varphi}{2 \pi f_c} \quad (4)$$

Upon substituting (3) into (4), we can obtain the expression for determining the measuring error of the range σD introduced by the ionosphere:

$$\sigma D = \frac{c \times 8.44 \times 10^{-7} \times dI}{2 \pi f_c^2} = 4.48 \times dI \quad (5)$$

As is seen from (5), the error σD is directly proportional to the TEC variation dI and inversely proportional to the carrier frequency squared.

Using the values of the spatial derivatives of TEC I'_x and I'_y and of the derivative of TEC with respect to time I'_t makes it possible to uniquely obtain - for each instant of time - the values of errors of determination of the angle of arrival $\sigma\alpha$ and the frequency Doppler shift σf by formulas (Kravtsov et al., 1983; Goodman and Aarons, 1990):

$$\sigma\alpha = \frac{1.39 \times 10^2}{f_c^2} \times \sqrt{(I'_x)^2 + (I'_y)^2} \quad (6)$$

$$\sigma f = \frac{1.34 \times 10^{-7}}{f_c} \times I'_t \quad (7)$$

In the simplest case, the values of the derivatives for the selected cell of the map can be obtained using TEC increments for the four cell nodes and for two times t_1 and $t_2 = t_1 + d_t$:

$$\begin{aligned} \Delta I &= (I_{a2} - I_{a1} + I_{b2} - I_{b1} + I_{c2} - I_{c1} + I_{d2} - I_{d1})/4 \\ \Delta I'_t &= (I_{a2} - I_{a1} + I_{b2} - I_{b1} + I_{c2} - I_{c1} + I_{d2} - I_{d1})/4d_t \\ \Delta I'_x &= (I_{c1} - I_{b1} + I_{d1} - I_{a1} + I_{c2} - I_{b2} + I_{d2} - I_{a2})/4d_e \\ \Delta I'_y &= (I_{a1} - I_{b1} + I_{d1} - I_{c1} + I_{a2} - I_{b2} + I_{d2} - I_{c2})/4d_n \end{aligned} \quad (8)$$

Where necessary, the spatial derivatives can be estimated by taking into account the TEC values in adjacent nodes of the map, and the time derivative (with a time resolution of IONEX maps no worse than 15 min) can be inferred by averaging increments for several successive time counts.

The procedures (5), (6) and (7) are performed for all cells of the selected spatial range and for the selected time interval of the day. One variant of data representation implies a full exploitation of the IONEX format with the difference that, rather than the values of TEC and the error of TEC determination (Schaer et al., 1998), are entered into the corresponding cells of the map values of error σD , σf and $\sigma\alpha$.

By way of example, it is appropriate to give the results derived from analyzing the regular part of the spatial-temporal TEC variations for a relatively magnetically quiet

day of July 29, 1999 (with the largest deviation of the D_{st} -index of -40 nT) and for the magnetically disturbed day of April 6, 2000 (with the largest deviation of the D_{st} -index of -293 nT).

Fig.3 a, b, c portrays the maps of the errors σD , σf and $\sigma \alpha$ obtained on the basis of files in the IONEX format for the magnetically quiet day of July 29, 1999 in the geographic coordinate system in the range of longitudes $-120^\circ \dots -60^\circ E$ and latitudes $20^\circ \dots 70^\circ N$. Fig.3 d, e, f, respectively, characterizes the values of σD , σf and $\sigma \alpha$ for the magnetically disturbed day of April 6, 2000. The figure also shows the time interval 19-21 UT, for which the analysis was carried out. Contours show the values of errors of phase measurements in units, respectively, of σD - "m" (meters), σf - "Hz" (Hertz), and $\sigma \alpha$ - "arcmin" (minutes of arc). The vertical calibrated scale shows the maximum and minimum values of the corresponding errors.

The above maps are a pictorial rendition of the behavior dynamics of the errors σD , σf and $\sigma \alpha$ in the spatial and temporal ranges selected. Noteworthy is a considerable difference of the maps for the magnetically quiet and disturbed days. As is evident from Fig.3, gradients of spatial distribution of the errors during disturbances increase more than an order of magnitude when compared to the quiet period, which would lead to a degradation of RESS performance.

5 Analysis of the irregular errors σD , σf and $\sigma \alpha$

Our analysis of the irregular component of the errors was based on using raw data in the form of series of TEC values for selected receiving sites as well as values of elevations $\Theta_s(t)$ and azimuths $\alpha_s(t)$ to visible satellites that were calculated using a specially developed program, CONVTEC, to convert RINEX-files (standard files for the GPS system) available from the Internet (Afraimovich et al., 1998a).

Fig.4 presents the geometry of transitionospheric radio sounding. The axes z, y, x are pointing, respectively, to the zenith, the north N , and to the east E ; P is the point of intersection of the LOS to the satellite (the line connecting the satellite to the radio signal receiver) with the ionospheric F_2 region peak; S is the subionospheric point (projection of the point P onto the terrestrial surface).

The GPS technology provides the means of estimating TEC variations on the basis of phase measurements of TEC I in each of the spaced two-frequency GPS receivers

using the formula (Hofmann-Wellenhof et al., 1992):

$$I_0 = \frac{1}{40.308} \frac{f_1^2 f_2^2}{f_1^2 - f_2^2} [(L_1 \lambda_1 - L_2 \lambda_2) + \text{const} + nL], \quad (9)$$

where $L_1 \lambda_1$ and $L_2 \lambda_2$ are phase path increments of the radio signal, caused by the phase delay in the ionosphere (m); L_1 and L_2 are the number of full phase rotations, and λ_1 and λ_2 are the wavelengths (m) for the frequencies f_1 and f_2 , respectively; *const* is some unknown initial phase path (m); and nL is the error in determination of the phase path (m). Phase measurements in the GPS can be made with a high degree of accuracy corresponding to the error of TEC determination of at least 10^{14} m^{-2} when averaged on a 30-second time interval, with some uncertainty of the initial value of TEC, however (Hofmann-Wellenhof et al., 1992). For definiteness sake, we bring the TEC variations into the region of positive values with the minimum value equal to 0 by adjusting the constant term *const* in equation (9). The TECU (Total Electron Content Units), which is equal to 10^{16} m^{-2} and is commonly accepted in the literature, will be used throughout the text.

Primary data include series of "oblique" values of TEC $I_o(t)$, as well as the corresponding series of elevations $\theta(t)$ and azimuths $\alpha(t)$ along LOS to the satellite calculated using our developed CONVTEC program which converts the GPS system standard RINEX-files on the Internet (Gurtner, 1993). Series of the values of elevations $\theta(t)$ and azimuths $\alpha(t)$ of the beam to the satellite were used to determine the coordinates of subionospheric points, and to convert the "oblique" TEC $I_o(t)$ to the corresponding value of the "vertical" TEC $I(t)$ by employing the technique reported by (Klobuchar, 1986):

$$I = I_0 \times \cos \left[\arcsin \left(\frac{R_z}{R_z + h_{max}} \cos \Theta_s \right) \right], \quad (10)$$

where R_z is the Earth's radius, and $h_{max}=300 \text{ km}$ is the height of the F_2 -layer maximum.

All results in this study were obtained for elevations $\Theta_s(t)$ larger than 30° .

To analyze the errors σD , σf and $\sigma \alpha$ that are caused by the irregular component of TEC variation, we make use of the relations for the respective regular errors (5), (6) and (7). The difference in the analysis of irregular errors implies a different (compared with the IONEX technique) method of determining the values of TEC and its derivatives (Afraimovich and Karachenschev, 2002b).

The phase differences $\Delta\varphi_{x,y}$ along the axes x and y are proportional to the values of the horizontal components of TEC gradient $G_E = I'_x$ and $G_E = I'_y$.

To calculate the components of the TEC gradient I'_x and I'_y are used linear transformations of the differences of the values of the filtered TEC ($I_B - I_A$) and ($I_B - I_C$) at the receiving points A , B and C (Afraimovich et al., 1998a):

$$I'_x = \frac{y_A(I_B - I_C) - y_C(I_B - I_A)}{x_A y_C - x_C y_A}; \quad I'_y = \frac{x_C(I_B - I_A) - x_A(I_B - I_C)}{x_A y_C - x_C y_A} \quad (11)$$

where x_A , y_A , x_C , y_C are the coordinates of the sites A and C in the topocentric coordinate system. When deriving (11) we took into account that $x_B = y_B = 0$, since site B is the center of topocentric coordinate system.

The time derivative of TEC I'_t is determined by differentiating $I(t)$ at the point B .

The procedures of (5), (6) and (7) are performed for all groups of three GPS stations of the selected spatial range and for satellites visible from these stations, as well as for the selected time interval of the day.

Fig.5 presents the results derived from analyzing the irregular component of the errors σD , σf and $\sigma \alpha$ in the form of fluctuation spectra of the range, Doppler frequency and angles of arrival of radio waves.

With the purpose of improving the statistical reliability of the data, we used the spatial averaging technique for spectra within the framework of a novel technology (Afraimovich et al., 2001a). The method implies using an appropriate processing of TEC variations that are determined from the GPS data, simultaneously for the entire set of GPS satellites (as many as 5–10 satellites) "visible" during a given time interval, at all stations of the global GPS network used in the analysis.

Individual spectra of the errors σD , σf and $\sigma \alpha$ were obtained by processing continuous series of $I(t)$ measurements of a duration no shorter than 2.5 hours. To eliminate errors caused by the regular ionosphere, as well as trends introduced the motion of satellites, we used the procedure of removing the linear trend by preliminarily smoothing the initial series with the selected time window of a duration of about 60 min.

Fig.5 shows the overall character of the TEC variations $dI(t)$ that were filtered from TEC series obtained from measurements of the phase difference between two coherently coupled signals from the GPS system (Hofmann-Wellenhof, 1992) for the magnetically quiet day of July 29, 1999 (panel a , at the left) and a major magnetic storm of July 15, 2000 (panel b , at the right). Furthermore, the panels show the station names and

locations, as well as GPS satellite numbers (PRN). In this paper we are using the term PRN (pseudo random noise) to designate the satellite number (Hofmann-Wellenhof et al., 1992).

As is evident from the figure, the intensity $dI(t)$ during the disturbance even at such low latitudes is increased an order of magnitude as a minimum. This is reflected on logarithmic amplitude spectra $lgS(F)$ of TEC fluctuations and their derivatives (left-hand scale in the figures) and of the fluctuations of σD , σf and $\sigma \alpha$, converted to the working frequency of 300 MHz (right-hand scale) which are represented on a logarithmic scale (panels *b*, *c*, *d*, *f*, *g*, *h*).

The logarithmic amplitude spectrum $lgS(F)$ obtained by using a standard FFT procedure. Incoherent summation of the partial amplitude spectra $lgS(F)_i$ of different LOS was performed by the formula:

$$lg\langle S(F) \rangle = lg \left[\frac{\sum_{i=1}^n S(F)_i}{n} \right] \quad (12)$$

where i is the number of LOS; $i = 1, 2, \dots, n$.

As a consequence of the statistical independence of partial spectra, the signal/noise ratio, when the average spectrum is calculated, increases due to incoherent accumulation at least by a factor of \sqrt{n} , where n is the number of LOS.

Fluctuation spectra from the magnetically quiet day of July 29, 1999 are shown by the thin line in panels *f*, *g*, *h* (Fig.5) for comparison with the spectra from the disturbed day. The range of fluctuation periods is shown in bold type along the abscissa axis in panels *d* and *h*. Panels *b* and *f* show also the number n of GPS arrays composed of three stations, the data from which are used to estimate the spatial derivatives of TEC (Afraimovich et al., 2001a).

Spectra of phase fluctuations have a power law character with the values of the slopes ν , shown in panels *b*, *c*, *d*, *f*, *g*, *h*. The slope of spectrum is determined by the slope of the fitted straight line (thin black line in panel *b* of Fig.5). These results are in reasonably good agreement with data reported in Komrakov and Skrebkova, 1980; Livingston et al., 1981; Gajlit et al., 1983; Kravtsov et al., 1983; Gershman et al., 1984; Yakubov, 1997).

6 The method of GPS phase slips estimates

The study of deep, fast variations in TEC caused by a strong scattering of satellite signals from intense small-scale irregularities of the ionospheric $F2$ -layer at equatorial and polar latitudes has a special place among ionospheric investigations based on using satellite (including GPS) signals (Aarons, 1982; Basu et al., 1988; Aarons et al., 1996, 1997; Pi et al., 1997; Aarons and Lin, 1999; Bhattacharrya et al., 2000; Shan et al., 2002). The interest to this problem as regards the practical implementation is explained by the fact that as a result of such a scattering, the signal undergoes deep amplitude fadings, which leads to a phase slip at the GPS working frequencies (Skone and Jong, 2000, 2001).

A limitation of the cited references is the fact that they use, as input data, essentially the values of TEC determined from the phase difference $L1 - L2$ (see below). For that reason, fatal phase slips that totally prohibit measurements of continuous TEC variations, are excluded from the sample statistic reported in the cited references.

In this section we inquire into the question: What is the statistic of fatal phase slips, and how it depends on the various geophysical factors (the level of geomagnetic disturbance, the latitudinal and diurnal dependencies)?

The purpose of a preprocessing of the GPS data is to obtain slip density estimates in measuring the phase difference $L1 - L2$, and slips of phase measurement at the fundamental frequency $L1$. Ascertaining the cause of the increase in slip density was also greatly facilitated by estimating the TEC variation intensity for the same stations and time intervals.

6.1 The relative density of difference phase $L1 - L2$ slips and of phase $L1$ slips

The GPS technology provides the means of estimating TEC variations on the basis of phase measurements of TEC I in each of the spaced two-frequency GPS receivers using the formula (9). We hold fixed a slip of the phase difference $L1 - L2$ in the case where the modulus of the TEC increment for a time interval of 30 s (which is a standard one for the GPS data placed on the Internet), exceeds the specified threshold of order, for example, 100-200 TECU. A slip of phase $L1$ is also fixed in a similar manner but with a much larger threshold and with due regard for the time varying distance to the

satellite.

Thus we point out that it is the fatal slips which totally prohibit the determination of the increment of TEC from the measures value of the phase difference $L1 - L2$. At the same time there can be numerous phase slips whose absolute value is smaller than the threshold which we selected. Such slips that accompany TEC variations of only a few TECU, are caused by ionospheric irregularity effects, and have been thoroughly studied in a large number of publications (Basu et al., 1988; Aarons et al., 1996, 1997; Pi et al., 1997; Aarons and Lin, 1999; Bhattacharrya et al., 2000).

As a result of a pretreatment of the RINEX-files, we have the number S of phase slips within a single selected time interval $dT=5$ min, as well as the corresponding number M of observations that is required for normalizing the data. These data for each of the GPS satellites were then averaged for all the stations selected in order to infer the mean density of observations $M(t)$ and the mean density of phase slips $S(t)$. In the middle of the observed satellite pass, the density of observations $M(t)$ averages 10 ± 1 (30-s counts); at the beginning and end of the pass it can decrease because the time intervals of observation of a given satellite at elevations larger than that specified do not coincide at different stations. Subsequently, we calculated the mean relative density of phase slips $P(t)=S(t)/M(t)$, %. Furthermore, the daily mean value of the relative number of phase slips $\langle P \rangle$ that was averaged over all GPS satellites and stations was useful for our analysis.

As would be expected the mean observation density $M(t)$ for a single satellite exhibits a diurnal variation that is determined by the satellite's orbit, and varies over the range from 0 to 8.

6.2 Estimation of the TEC variation intensity

We have used the series $I(t)$, containing neither slips of the phase difference $L1 - L2$ nor gaps of counts, to estimate the TEC variation intensity for the same sets of stations and time intervals as used in estimating the phase slip density.

To exclude the variations of the regular ionosphere, as well as trends introduced by the motion of the satellite, we employ the procedure of removing the linear trend by preliminarily smoothing the initial series with a selected time window of a duration of about 60 min. In a subsequent treatment, we use the standard deviation of the TEC variations $dI(t)$, thus filtered, as an estimate of the TEC variation intensity A (see

Section 4).

Fig.6a gives an example of a typical weakly disturbed variation in "vertical" TEC $I(t)$ for station WES2 (42.6°N , 288.5°E); satellite number PRN10 on July 15, 2000 for the time interval 14:00–16:00 UT, preceding the onset of a geomagnetic disturbance near the WES2 station. For this same series, Fig.6b presents the $dI(t)$ variations that were filtered out from the $I(t)$ series (rms of $dI(t)$ is smaller than 0.2 TECU).

Strong variations in TEC variation intensity occurred near station WES2 literally within 6 hours. Fig.6e and Fig.6f presents the dependencies $I(t)$ and $dI(t)$ for station WES2 for the time interval 20:00–22:00 UT (PRN23). As is evident from the figure, the TEC variations increased in intensity at least by a factor of 30 when compared with the time interval 14:00–16:00 UT (Fig.6a and Fig.6b).

6.3 Conditions and limitations of a data processing

Slips of phase measurements can be caused by reception conditions for the signal in the neighborhood of the receiver (interference from thunderstorms, radiointerferences), which is particularly pronounced at low elevations θ . To exclude the influence of the signal reception conditions, in this paper we used only observations with satellite elevations θ larger than 30° .

Since we are using a global averaging of the number of phase slips for all LOS's and stations, as a consequence of the uneven distribution of stations the proportion of mid-latitude stations of North America and, to a lesser extent, of Europe is predominant (see above). At the same time the number of stations in the polar region of the northern hemisphere and in the equatorial zone was found to be quite sufficient for a comparative analysis. To compare the results, we chose 3 latitude ranges: high latitudes $50 - 80^{\circ}\text{N}$; mid-latitudes $30 - 50^{\circ}\text{N}$; and equatorial zone $30^{\circ}\text{S} - 30^{\circ}\text{N}$.

We selected also the data according to the types of two-frequency receivers, with which the GPS global network sites are equipped (the relevant information is contained in the initial RINEX format).

7 Results derived from analyzing the relative density of phase slips

7.1 Magnetically quiet days

Fig.7 plots the local time LT-dependence of the relative mean slip density $P(t)$ obtained by averaging the data from all satellites in the latitude range $0 - 360^\circ\text{E}$ irrespective of the type of GPS receivers for the magnetically quiet days of July 29, 1999 (at the left) and January 9, 2000 (at the right). The local time for each GPS station was calculated, based on the value of its geographic longitude. The number n of satellite passes used to carry out an averaging is marked in all panels.

As is evident from Fig.7b, the phase slips on a magnetically quiet day at mid-latitudes have a sporadic character. The daily mean value of the relative density of phase slips $\langle P \rangle$, averaged over all GPS satellites and stations, was 0.017 % for the magnetically quiet day of July 29, 1999. Similar data were also obtained for high latitudes (Fig.7a).

In the equatorial zone, however, even on a magnetically quiet day, the density of phase slips exceeds the latitudinally mean value of $P(t)$ at least by a factor of 15, and shows a strongly pronounced LT-dependence, with a maximum value of 1.52 % (Fig.7c).

For the other magnetically quiet day of January 9, 2000, however, the mean value of $\langle P \rangle$ at mid-latitudes was already larger 0.06 % (Fig.7e). For the diurnal $P(t)$ -dependence on January 9, 2000, one can point out the irregularity of the mean density of phase slips as a function of local time LT.

7.2 Magnetic storms of April 6 and July 15, 2000

A totally different picture was observed on April 6, 2000 during a strong magnetic storm with a well-defined SSC.

Fig.8 presents the measured variations of the H -component of the geomagnetic field at station Irkutsk (52.2°N ; 104.3°E –a, e), and Dst (b, f - thick line) during major magnetic storms on April 6, and July 15, 2000. The SSC times 16:42 UT and 14:37 UT are shown by a vertical bar.

Fig.8d (thick line) presents the variations of the UT-dependence of the relative

mean slip density $P(t)$ obtained for the territory of North America ($200 - 300^\circ\text{E}$) at mid-latitudes $30 - 50^\circ\text{N}$ by averaging the data from all satellites. In this case, with the purpose of achieving a clearer detection of the effect of the magnetic storm SSC influence on the $P(t)$ -dependence, we chose only those GPS stations which were on the dayside of the Earth at the SSC time (North America region). Noteworthy is a well-defined effect of an increase in the density of phase slips that occurred after SSC.

A maximum mean slip density $P_{max}=2.4\%$ is attained 3-4 hours after an SSC. The same values, averaged over all observed satellites and mid-latitude stations ($0 - 360^\circ\text{E}$) but as a function of local time LT, are plotted in Fig.9b.

First of all, it should be noted that the relative density of phase slips $P(t)$ exceeds that for magnetically quiet days by one (when compared with January 9, 2000) or even two (when compared with July 29, 1999) orders of magnitude, and reaches a few percent of the total observation density. The mean value of $\langle P \rangle$ for this storm is 0.67 %, which is by a factor of 40 larger than that of $\langle P \rangle$ for July 29, 1000, and by a factor of 10 larger than that for January 9, 2000.

It was also found that the averaged (over all satellites) level of phase slips for the GPS satellites on the subsolar side of the Earth is by a factor of 10 larger than that on the opposite side of the Earth (Fig.9b).

Similar dependencies with a maximum slip density $P_{max}=3.37\%$ and a sharply pronounced diurnal dependence were also obtained for equatorial latitudes (Fig.9c). On the other hand, although the high latitudes show a 10-fold growth of $\langle P \rangle$ as against a magnetically quiet day, no LT-dependence is observed (Fig.9a).

A similar result confirming all of the above-mentioned features of the April 6, 2000 storm was also obtained for the other magnetic storm of July 15, 2000 (see the universal time UT dependence in Fig.8h and the local time LT dependencies of the relative mean density of phase slips $P(t)$ obtained by averaging the data from all GPS satellites, in Fig.9d, e, f.

The mean value of $\langle P \rangle$ for this storm at mid-latitudes is 0.34 %, which is also in appreciable excess of the level of phase slips for magnetically quiet days ($P_{max}=4\%$). The effect of an increase in the density of phase slips after SSC is clearly pronounced for this storm as well (Fig.8h, thick line; see below).

These results are in reasonably good agreement with data reported by Coster et al. (2001). This authors presented the regional GPS mapping of storm enhanced density

during the July 15-16 2000 geomagnetic storm and found, that the Millstone GPS receiver ASHTECH Z-12 lost (and then regained) lock on all satellites between 20.40 and 24.00 UT.

7.3 Correlation of the increase in slip density and TEC variation intensity

It is known that equatorial latitudes are characterized by strong scintillations of the transitionospheric signal caused by the scattering from *F*2-region ionization irregularities (Aarons, 1982; Basu et al., 1988; Aarons et al., 1996, 1997; Pi et al., 1997; Aarons and Lin, 1999; Bhattacharrya et al., 2000).

Since during the active phase of the magnetic storm the mid-latitude ionosphere becomes increasingly inhomogeneous, it might be anticipated that a similar mechanism is able to cause appreciable scintillations of the GPS signal at mid-latitudes as well. To verify this hypothesis, we determined the dependencies $A(t)$ of the TEC variation intensity obtained for the same set of stations as in the case of $P(t)$.

The dependencies $A(t)$ as a function of UT (Fig.8d, h - dashed line) and LT (Fig.9b, e - dashed line) presented below by averaging (over all GPS satellites and stations) the standard deviation of the variations $dI(t)$ (Afraimovich et al., 2001a).

In Fig.8h, the dashed line represents the dependence $A(t)$ of the TEC variation intensity obtained for all satellites and for the territory of North America at mid-latitudes $30 - 50^{\circ}\text{N}$ during the magnetic storm of July 15, 2000. As is apparent from this figure, the dependence $A(t)$ correlates quite well with the UT-dependence of the relative mean slip density $P(t)$ calculated from the same set of stations as in the case of $A(t)$.

A similar result on the UT-dependence was also obtained for a major magnetic storm of April 6, 2000 (Fig.8d, dashed line). A correlation of the increase in slip density and in TEC variation intensity is shown as clearly by the LT-dependencies $A(t)$ for the magnetic storms of April 6 and July 15, 2000, presented in Fig.9b, e (dashed line).

The fact was found that the growth of the level of geomagnetic activity is accompanied by the growth of total intensity $A(t)$ of TEC variations in the range of 20-60 min periods (traveling ionospheric disturbances, TIDs); however, it shows correlation not with the absolute level of Dst , but with the value of the time derivative of Dst (the

maximum correlation coefficient reaches 0.94 – Fig.8b, f, dashed line). The derivative $d(Dst)/dt$ was obtained from the dependence $Dst(t)$ (Fig.8b, f, dashed line). The delay of the TID response about 2 hours is consistent with the guess that TIDs are generated in auroral regions, and propagate equator-ward with approximate velocity of 300-400 m/s (Hocke and Schlegel, 1996; Oliver et al., 1997; Afraimovich et al., 1998b; 2002e).

7.4 The dependence of the slip density of phase measurements $L1 - L2$ and $L1$ on the type of GPS receivers

We have carried out an analysis of the dependence of the density of fatal slips on the type of GPS receivers; furthermore, we have verified slips for which of the channels ($L1$ or $L2$) are the cause of slips in measurements of the phase difference $L1 - L2$.

The sample statistic of phase slips for the main types of two-frequency receivers (ASHTECH, TRIMBLE, AOA), installed at the global GPS network sites, is presented in Fig.10 and Fig.11.

An analysis of slips in measuring the phase difference $L1 - L2$ and of the phase $L1$ was carried out for the magnetic storms of April 6, and July 15, 2000.

Fig.10 plots the UT-dependencies of the relative mean slip density $P(t)$ of phase measurements of $L1 - L2$ (at the left) and phase measurements of $L1$ only (at the right) obtained by averaging the data from all satellites in the longitude range $200 - 300^\circ E$ at the mid-latitudes $30 - 50^\circ N$ for major magnetic storm on April 6, 2000.

The data from Fig.10a suggest that for the ASHTECH receivers, the slip density of phase measurements at two frequencies $L1 - L2$ is by a factor of 5-20 smaller than that for the other types of receivers. These estimates are only slightly exceeded by the slip density for the TRIMBLE receivers (Fig.10b). The AOA receivers are the most susceptible to slips of $L1 - L2$ measurements (Fig.10c). The mean and maximum values of $P(t)$ exceed the respective values for the ASHTECH receivers during the magnetic storm of April 6, 2000, at least by a factor of 10-20.

Fig.11 plots the UT-dependencies of the relative mean slip density $P(t)$ of phase measurements of $L1 - L2$ (at the left) and phase measurements of $L1$ only (at the right) obtained by averaging the data from all satellites in the longitude range $0 - 360^\circ E$ at the equatorial zone $30^\circ S - 30^\circ N$ for major magnetic storm on April 6, 2000.

The statistic of the $L1 - L2$ slips for the AOA and TRIMBLE receivers differ almost not at all from the data for mid-latitudes. For the ASHTECH receivers, however, the

density of slips in the equatorial zone was found to be little lower when compared with the AOA receivers.

On the other hand, the level of slips of $L1$ phase measurements at the fundamental GPS frequency (Fig.8d, h and Fig.10 and Fig.11, at the right) is at least one order of magnitude lower than that in $L1 - L2$ measurements.

The corresponding dependencies $P(t)$ as a function of universal time UT on the dayside for the magnetic storms of April 6 and July 15, 2000, are plotted in Fig.8c and g, respectively. Although the level of the slips is lower by one order of magnitude (as compared to $P(t)$ for $L1 - L2$ - panels d and h), the fundamental frequency $L1$ does show an increase in the relative density of slips in the main phase of the magnetic storm.

Similar results of a comparison of the level of $L1 - L2$ and $L1$ slips for different types of GPS receivers were also obtained for the magnetic storm of July 15, 2000.

This leads us to conjecture that the slips of $L1 - L2$ measurements are most likely to be caused by the high level of slips of $L2$ phase measurements at the auxiliary frequency. According to our data, these slips are observed at equatorial latitudes under quiet conditions as well, and at mid-latitudes they increase with increasing geomagnetic activity.

This means that relatively long-term (about 10 years) data from the global GPS network equipped with several hundred older-generation commercial receivers cannot be exploited in full measure to obtain data on TEC variations, based on a standard processing of the phase difference $L1 - L2$. This limitation is legitimate for the period of the main phase of the magnetic storm and of the dayside ionosphere which is characterized by fast, profound TEC variations.

7.5 Determination of TEC variations at the fundamental frequency $L1$

Some way out of the situation would be by exploiting the method (Afraimovich et al., 1998a) for determining TEC variations using only the data on the pseudo-range C and phase measurements at the fundamental frequency $L1$. In this study the concerned method was tested with the database mentioned in Table 1.

For testing purposes, time intervals were chosen with no data gaps and slips of phase slip measurements of both $L1 - L2$ and $L1$.

Phase changes at frequencies f_1 and f_2 may be represented as the sum of different components $\phi_\Sigma = \phi_s + \phi + \phi_0$, where $\phi_s = 2\pi C/\lambda$ is the fundamental component caused by a change of the distance D to the satellite it follows its orbit; $\phi = 8,42 * 10^{-7}I/f$ is the ionospheric component proportional to TEC at LOS between the receiver and the satellite (Spoelstra and Kelder, 1984); and ϕ_0 is the initial phase. To subtract ϕ_s , it is possible to use current information about the pseudorange C for each satellite (Hofmann-Wellenhof et al., 1992).

For the sake of comparison with the $dI(t)$ variations obtained using the standard TEC measurement technique described in Section 3, from data on the phase difference $L1 - L2$ (Fig.6b, thick lines), dashed lines plot the variations of the "vertical" TEC value obtained by measuring the $L1$ phase and filtered off (as is done for the data on $L1 - L2$) by removing the trend with the 60-min time window. It is evident from the figure that the difference of the $dI(t)$ dependencies from each other does not exceed in magnitude the value 0.1 TECU, and is more pronounced only for the quiet period 14:00-16:00 UT.

For the disturbed time interval 20:00-22:00 UT (Fig.6f), the corresponding dependencies are virtually similar and are not distinguishable. Fig.6 presents also the distributions $P(\delta)$ of the standard deviation δ of TEC variations obtained in phase measurements at two frequencies $L1 - L2$ and at the fundamental frequency $L1$. Panels c, d, g and h show the time intervals and the number n of satellite passes, over which the averaging was performed.

During the quiet period 10:00-12:00 UT on April 6 and July 15, 2000 (Fig.6c, g), the most probable value of δ was 0.04 and 0.05 TECU, and was nearly twice as large as the corresponding value for the same time interval on the magnetically quiet day of July 29, 1999. Furthermore, the mean values of δ were by a factor of 1.2-1.5 larger than the most probable ones. For the disturbed period 20:00-22:00 UT (Fig.6d, h), the most probable value of δ remained virtually unchanged; however, the mean values of δ now were larger than the most probable ones by a factor of 2-3. This is indicative of a more significant discrepancy between results of a calculation of the $dI(t)$ variations from $L1 - L2$ and $L1$.

Thus the standard deviation of the TEC variations obtained in phase measurements at two frequencies $L1 - L2$ and at the fundamental frequency $L1$ does not exceed 0.1 TECU, which makes this method useful for strong disturbance conditions where slips

at the auxiliary frequency $L2$ are observed. Of course, this method is appropriate for solving only those problems, for which it will suffice to single out the TEC variations, and is unsuitable for calculating the absolute value of TEC.

8 Discussion and Conclusions

The main results of this study may be summarized as follows:

1. We found that during strong magnetic storms, the errors of determination of the range, frequency Doppler shift and angles of arrival of transionospheric radio signals exceeds the one for magnetically quiet days by one order of magnitude as a minimum. This can be the cause of performance degradation of current satellite radio engineering navigation, communication and radar systems as well as of superlong-baseline radio interferometry systems (Afraimovich and Karachenschev, 2002b).
2. We have detected a dependence of the relative density of phase slips in some GPS receivers on the disturbance level of the Earth's magnetosphere during major magnetic storms (Afraimovich et al., 2000c; 2001b; 2001c; 2001d; 2002a). During strong magnetic storms, the relative density of phase slips at mid latitudes exceeds its mean value for magnetically quiet days at least by the order of one or two, and reaches a few percent of the total density of observations. Furthermore, the level of phase slips for the GPS satellites located at the sunward side of the Earth was 5-10 times larger compared with the opposite side of the Earth.
3. The level of slips of $L1$ phase measurements at the fundamental GPS frequency is at least one order of magnitude lower than that in $L1 - L2$ measurements. The slips of $L1 - L2$ measurements are most likely to be caused by the high level of slips of $L2$ phase measurements at the auxiliary frequency (Afraimovich et al., 2000c; 2001b; 2001c; 2001d; 2002a).

As an alternative, Afraimovich et al. (2001b; 2001d) have developed and tested a new method for determining TEC variations using only data on the pseudo-range and phase measurements at fundamental frequency $L1$. The standard deviation of the TEC variations which were obtained in phase measurements at two frequencies, $L1 - L2$, and at fundamental frequency $L1$, does not exceed 0.1 TECU, which permits this method to be used in strong disturbance conditions when phase slips at auxiliary frequency $L2$ are observed.

4. However, the reason for the slips themselves can include several factors: the influence of additive interferences in the case of a low signal/noise ratio, the

signal scattering from electron density irregularities, and the inadequate response of GPS receivers of some types to fast changes in daytime TEC at the auxiliary frequency $L2$. Let us analyze these factors separately.

5. The lower signal/noise ratio at $L2$ is primarily due to the fact that the $L2$ power at the GPS satellite transmitter output is on 6 dB of magnitude smaller compared with the fundamental frequency f_1 using C/A code (ICD-200, 1994; Langley, 1998). Similar correlations of the effective radiated power of $L1$ (30 watt) and $L2$ (21 watt) signals are also characteristic for the Russian GLONASS system (Kharisov et al., 1998).

Phase slips at $L2$ can also be caused by the lower signal/noise ratio when use is made of commercial noncoded receivers for the frequency $L2$, with which the global GPS network stations are equipped. These receivers have no access to the military "Y" code, and have to use the noncoded or semi-noncoded mode of reception. As a consequence, the signal/noise ratio at the frequency $L2$ is, at best, by 13 dB lower compared to the mode of fully coded reception.

Thus the difference in signal powers at $L1$ and $L2$ for commercial receivers can become larger than 10 dB, which can lead to an increase of the level of $L2$ slips because of the influence of additive interferences. Different types of GPS receivers respond to this differently; on the whole, however, the picture of the dependence on the local time, latitude range, and on the level of geomagnetic activity remains sufficiently stable.

6. However, the deterioration of the signal/noise ratio with an increase of the level of geomagnetic disturbance is possible if this is accompanied by an enhancement of the proportion of the signal scattered from ionospheric electron density irregularities. This involves also an increase of the number of phase slips; for a more powerful $L1$ signal, however, the density of slips is an order of magnitude smaller than that for the less powerful $L2$ signal.

The high positive correlation between the growth of the density of phase slips $P(t)$ and the intensity of ionospheric irregularities $A(t)$ during geomagnetic disturbances as detected in this study points to the fact that the increase in slips $P(t)$ is caused by the scattering of the GPS signal from ionospheric irregularities.

Nevertheless, the presence of the daytime maximum in the diurnal density distribution of fatal slips and of the TEC variation amplitude is inconsistent with existing data on the night-time intensity maximum of equatorial scintillations of transitionospheric signals (Aarons, 1982; Aarons et al., 1996, 1997; Pi et al., 1997; Aarons and Lin, 1999). Besides, the level of slips at mid-latitudes was found to be unusually high.

This would suggest that the reason for the increase in density of fatal phase slips during geomagnetic disturbances is that the type of GPS signal scattering from ionospheric irregularities is different from that causing signal scintillations in the case of the scattering from *F* region irregularities at the local night-time in the equatorial zone.

The probable phenomenon that is responsible for the phase slips would be the effect of a strong resonance backscatter of the signal from field-aligned irregularities in the *E*-region of ionosphere (Foster and Tetenbaum, 1991). Such a scattering can lead to strong signal fadings, and even to a particle screening of the "GPS satellite - receiver" propagation path.

Using the geomagnetic storm of July 15, 2000 as an example, Afraimovich et al. (2001c) investigated the dependence of GPS navigation system performance on the nightside at mid-latitudes on the level of geomagnetic disturbance. It was shown that the number of GPS phase slips increases with the increasing level of disturbance and that there is a good correlation between the rate of *Dst*-variation and the frequency of slips. It was further shown that the relative frequency of slips has also a clearly pronounced aspect dependence. Phase slips of the GPS signal can be caused by the scattering from small-scale irregularities of the ionospheric *E*-layer. Phase slip characteristics are indicative of Farley-Buneman instabilities as a plausible physical mechanism that is responsible for the formation of geomagnetic field-aligned irregularities (Foster and Tetenbaum, 1991). Using simultaneous measurements of backscatter signal characteristics from the Irkutsk incoherent scatter radar (Kurkin et al., 1999) and existing models for such irregularities, Afraimovich et al., (2001c) estimated the order of magnitude of the expected phase fluctuations of the GPS signal at a few degrees.

7. The increase in density of fatal slips during geomagnetic disturbances on the dayside can also be caused by limitations of the design and adjustment of the receivers used in the analysis, rather than the GPS signal scattering from ionospheric irregularities. An increase in slip density can be caused in this case by an inadequate response of GPS receivers of some types (such as AOA Turbo Rogue) to fast changes in daytime TEC at the auxiliary frequency *L2*. This effect prevents the identification of slips caused by phase fluctuations induced by the scattering from electron density irregularities. Unfortunately, we are unaware of any consistent investigation of this kind or published data lending support to such a point of view.

Of course, phase measurements are more sensitive to equipment failures and to various interference affecting GPS 'satellite-receiver' channel when compared with group delay measurements which are directly used for navigation purposes.

Therefore, it is necessary to have a monitoring of the errors of determining the position of stationary sites of the global GPS network, based on the data in the RINEX-format available from the Internet, and to analyze these series in conjunction with the data on the conditions of the near-terrestrial space environment.

Afraimovich et al. (2002c) found, that the rms error of positioning accuracy increases in the case where two-frequency GPS receivers of three main types (Ashtech, Trimble, and AOA) are in operation. For Ashtech receivers (unlike AOA and Trimble) there is also a clear correlation between the slip density of the one- and two-frequency modes of positioning and the level of geomagnetic disturbance.

As a result of our investigations, it has become clear that ionospheric disturbances during magnetic storms contribute to signal degradation and GPS system malfunctions not only at the equator and in the polar zone but also even at mid-latitudes. However, the question of the causes and the particular mechanisms of this influence remains largely open. The major objective of future research is to study the physical mechanisms of multi-scale total electron density variations in the ionosphere during geomagnetic disturbances of geospace that are accompanied by signal degradation and malfunctions of satellite radio engineering systems.

Such investigations must have a comprehensive character, with the maximum possible involvement of environmental ionospheric monitoring facilities (diverse ionospheric

herent scatter radars, chirp-ionosondes, etc.).

We are aware that this study has revealed only the key averaged patterns of this influence, and we hope that it would give impetus to a wide variety of more detailed investigations.

ACKNOWLEDGMENTS

The authors are grateful to V.A. Karachenschev, O.S. Lesuta, S.V. Voeykov and I.I. Ushakov for their active participation in investigations. The author are also indebted to E.A. Kosogorov, and O.S. Lesuta for preparing the input data. Thanks are also due V.G. Mikhalkovsky for his assistance in preparing the English version of the *TeX*manuscript. This work was done with support from the Russian Foundation for Basic Research (grants 00-05-72026 and 02-05-64570) and from RFBR grant of leading scientific schools of the Russian Federation 00-15-98509.

References

- [1] Aarons, J. Global morphology of ionospheric scintillations. *Proceedings of the IEEE*, 70(4), 360–378, 1982.
- [2] Aarons, J., Mendillo, M., Kudeki, E., and Yantosca, R. GPS phase fluctuations in the equatorial region during the MISETA 1994 campaign. *J. Geophys. Res.*, 101, 26851–26862, 1996.
- [3] Aarons, J., Mendillo, M., and Yantosca, R., GPS phase fluctuations in the equatorial region during sunspot minimum. *Radio Sci.*, 32, 1535–1550, 1997.
- [4] Aarons, J., and Lin, B. Development of high latitude phase fluctuations during the January 10, April 10-11, and May 15, 1997 magnetic storms. *J. Atmos. Terr. Phys.*, 61, 309–327, 1999.
- [5] Afraimovich, E. L., A. I. Terekhov, M. Yu. Udobov, and S. V. Fridman, Refraction distortions of transionospheric radio signals caused by changes in a regular ionosphere and by travelling ionospheric disturbances, *J. Atmos. and Terr. Phys.*, 54, 1013–1020, 1992.
- [6] Afraimovich, E. L., Palamartchouk, K. S. and Perevalova, N. P., GPS radio interferometry of travelling ionospheric disturbances. *J. Atmos. and Solar-Terr. Phys.*, 60, N. 12, 1205–1223, 1998a.
- [7] Afraimovich, E.L., E.A. Kosogorov, L.A. Leonovich, K.S. Palamarchouk, N.P. Perevalova, and O.M. Pirog. Determining parameters of large-scale traveling ionospheric disturbances of auroral origin using GPS-arrays. *J. Atm. Terr. Phys.*, 62, N7, 553–565, 1998b.
- [8] Afraimovich E.L., The GPS global detection of the ionospheric response to solar flares. *Radio sci.*, 35, N6, 1417–1424, 2000a.
- [9] Afraimovich, E.L., Chernukhov, V.V., Demyanov, V.V. Updating the ionospheric delay model for single-frequency equipment of users of the GPS. *Radio Sci.*, 35(1), 257–262, 2000b.

[10] Afraimovich, E.L., Lesyuta, O.S., Ushakov, I.I. Magnetospheric disturbances, and the GPS operation. LANL e-print archive, <http://xxx.lanl.gov/abs/physics/0009027>, 2000c.

[11] Afraimovich, E. L., Kosogorov, E. A., Lesyuta, O. S., Yakovets, A. F., Ushakov, I. I., Geomagnetic control of the spectrum of traveling ionospheric disturbances based on data from a global GPS network. *Ann. Geophys.*, 19, N. 7, 723–731, 2001a.

[12] Afraimovich, E.L., Lesyuta, O.S., and Voeykov, S.V. GPS phase slips on L1-L2 and L1 frequencies during geomagnetic disturbances. Proceedings of International Beacon Satellite Symposium, June 4-6, 2001, Boston College, Institute for Scientific Research, Chestnut Hill, MA, USA, 191–195, 2001b.

[13] Afraimovich, E.L., Berngardt, O.I., Lesyuta, O.S., Potekhin, A.P., and Shpynev, B.G. A Case Study of The Mid-Latitude GPS Performance at Nighttime During The Magnetic Storm of July 15, 2000. Proceedings of International Beacon Satellite Symposium, June 4-6, 2001, Boston College, Institute for Scientific Research, Chestnut Hill, MA, USA , 408–412, 2001c.

[14] Afraimovich, E.L., Lesyuta, O.S., Ushakov, I.I., and Voeykov, S.V. Geomagnetic storms and the occurrence of phase slips in the reception of GPS signals. *Annals of Geophysics*, 45(1), 55–71, 2001d.

[15] Afraimovich, E.L., E.A. Kosogorov, N.P. Perevalova, and A.V. Plotnikov. The use of GPS-arrays in detecting shock-acoustic waves generated during rocket launchings. *J.Atm. Solar-Terr. Phys.*, 63, N18, 1941–1957, 2001e.

[16] Afraimovich, E.L., A.T. Altyntsev, E.A. Kosogorov, N.S. Larina, and L.A. Leonovich. Ionospheric effects of the solar flares of September 23, 1998 and July 29, 1999 as deduced from global GPS network data. *J.Atm. Solar-Terr. Phys.*, 63, N17, 1841–1849, 2001f.

[17] Afraimovich, E.L., N.P. Perevalova, A.V. Plotnikov and A.M. Uralov. The shock-acoustic waves generated by the earthquakes. *Annales Geophysicae*, 19, N4, 395–409, 2001g.

- [18] Afraimovich, E.L., Lesyuta, O.S., and Ushakov, I.I. Geomagnetic disturbances, and the GPS operation. *Geomagnetism and Aeronomy*, 42(2), 220–227, 2002a.
- [19] Afraimovich E.L., Karachenschev V.A. Testing of the transitionospheric radiochannel using data from the global GPS network. LANL e-print archive, <http://xxx.lanl.gov/abs/physics/02100048>, 2002b.
- [20] Afraimovich E.L., Demyanov V.V., Kondakova T.N. Degradation of GPS performance in geomagnetically disturbed conditions. LANL e-print archive, <http://xxx.lanl.gov/abs/physics/0211015>, 2002c.
- [21] Afraimovich, E.L., E.A. Kosogorov and O.S. Lesyuta. Effects of the August 11, 1999 total solar eclipse as deduced from total electron content measurements at the GPS network. *J. Atm. Solar-Terr. Phys.*, 64/18, 1915–1923, 2002d.
- [22] Afraimovich, E. L., Ashkaliev, Ya. F., Aushev, V. M., Beletsky, A. B., Vodyanikov, V. V., Leonovich, L. A., Lesyuta, O. S., Mikhalev, A. V. and Yakovets, A. F. Radio and optical observations of large-scale traveling ionospheric disturbances during a strong geomagnetic storm of 6-8 April 2000. *J. Atm. Solar-Terr. Phys.*, 64/18, p.1971-1983, 2002e.
- [23] Basu Santimay, MacKenzie E., and Basu Sunanda. Ionospheric constraints on VHF/HUF communications links during solar maximum and minimum periods. *Radio Sci.*, 23, 363–378, 1988.
- [24] Bhattacharrya, A., Beach, T. L., Basu, S., and Kintner, P. M. Nighttime equatorial ionosphere: GPS scintillations and differential carrier phase fluctuations. *Radio Sci.*, 35, 209–224, 2000.
- [25] Coster, A.J., Foster, J.C., Erickson, P.J., Rich, F.J. Regional GPS Mapping of Storm Enhanced Density During the July 15-16 2000 Geomagnetic Storm. *Proceedings of International Beacon Satellite Symposium*, June 4-6, 2001, Boston College, Institute for Scientific Research, Chestnut Hill, MA, USA, 176–180, 2001.
- [26] Davies, K., *Ionospheric Radio Waves*. Blaisdell, Waltham, Mass., 1969.
- [27] Foster J.C. and Tetenbaum D., High resolution backscatter power observations of 440-MHz E-region coherent echoes at Millstone-Hill. *J. Geophys. Res.* 96, 1251–, 1991.

[28] Gajlit, T. A., Gusev, V. D., Erukhimov, L. M., Shapiro, P. I., Spectrum of the phase fluctuations at the ionosphere sounding. *Izv. Vuzov. Radiofizika*, 26, N. 7, 795–801, 1983.

[29] Gershman, B. N., Erukhimov, L. M. and Yashin, Yu. Ya. Wave Phenomena in the Ionosphere and Space Plasma. Moscow: Nauka, 1984, p. 392.

[30] Goodman, Dj. M., Aarons, J. Ionospheric Effects on Modern Electronic System. *Proceedings of the IEEE*, 78(3), 512–528, 1990.

[31] Gurtner, W. RINEX: The Receiver Independent Exchange Format Version 2, <http://igscb.jpl.nasa.gov/igscb/format/rinex2.txt>, 1993.

[32] Hocke, K., and K. Schlegel, A review of atmospheric gravity waves and traveling ionospheric disturbances: 1982-1995, *Ann. Geophys.*, 14, 917–940, 1996.

[33] Hofmann-Wellenhof, B., Lichtenegger, H. and Collins, J., Global Positioning System: Theory and Practice. it Springer-Verlag, New York, 1992, p.327.

[34] Ho, C.M., Mannucci, A.J., Linqwister, U. J. et al. Global ionosphere perturbations monitored by the worldwide GPS network. *Geophys. Res. Lett.*, 23(22), 3219–2222, 1996.

[35] Interface Control Document, ICD-200c, 1994.
<http://www.navcen.uscg.mil/pubs/gps/icd200/>.

[36] Langley, R. B. GPS for Geodesy. Springer: Berlin, Heidelberg, New York, Barcelona, Budapest, Hong Kong, London, Milan, Paris, Singapore, Tokyo, 1998.

[37] Kharisov, V. N., Perov, A. I., and Boldin, V. A. The Global Satellite Radio Navigation GLONASS System. Russia, Moscow: IPRZhR, 1998.

[38] Klobuchar, J. A., Ionospheric time-delay algorithm for single-frequency GPS users, *IEEE Transactions of Aerospace and Electronic System*, AES, 23, N. 3, 325–331, 1986.

[39] Kolosov, M. A., Armand, N. A. and Yakovlev, O. I. The Propagation of Radio Waves in Space Communication. Moscow: Svyaz, 1969, p. 155.

[40] Komrakov, G. P., Skrebkova, L. A., Study of parameters of ionospheric irregularities by the "Interkosmos-Kopernik 500" satellite. Ionosfernie issledovaniya, Moscow: Sovetskoe radio, 30, 49–52, 1980.

[41] Kravtsov, A. Yu., Feizulin, Z. I. and Vinogradov, A. G. The Propagation of Radio Waves Through the Earth's Ionosphere. Moscow: Radio i svyaz, 1983, p. 224.

[42] Kurkin V. I., Potekhin A. P., Shpynev B. G., Zarudnev V. E. and Zherebtsov G. A., Study of September 25, 1998 storm effects in the mid-latitude ionosphere using the Irkutsk Incoherent Scatter Radar. XXIV GA URSI (Abstracts). Toronto, Canada,, 441, 1999.

[43] Livingston, R. C., Rino, C. L., McClure, J. P., Hanson, W. B., Spectral characteristics of medium-scale equatorial F region irregularities, *J. Geophys. Res.*, 86, 2421–2428, 1981.

[44] Mannucci, A. J., Wilson, B. D., Yuan, D. N., Ho, C. M., Lindqwister, U. J. and Runge, T. F., A global mapping technique for GPS-driven ionospheric TEC measurements. *Radio Sci.*, 33, 565–582, 1998.

[45] National Space Weather Program. The Implementation Plan. 1997. Washington, DC, <http://www.ofcm.gov/nswp-ip/text/cover.htm>.

[46] Oliver, W. L., Otsuka Y., Sato M., Takami T., and Fukao, S. A climatology of F region gravity waves propagation over the middle and upper atmosphere radar. *J. Geophys. Res.*, 102, 14449-14512, 1997.

[47] Pi, X., Mannucci, A. J., Lindqwister, U. J., and Ho, C. M. Monitoring of global ionospheric irregularities using the worldwide GPS network. *Geophys. Res. Lett.*, 24, 2283–2286, 1997.

[48] Shaer et al. Global and Regional Ionospheric model using GPS double difference phase observable. IGS worksh. Proc. 77–91, 1997.

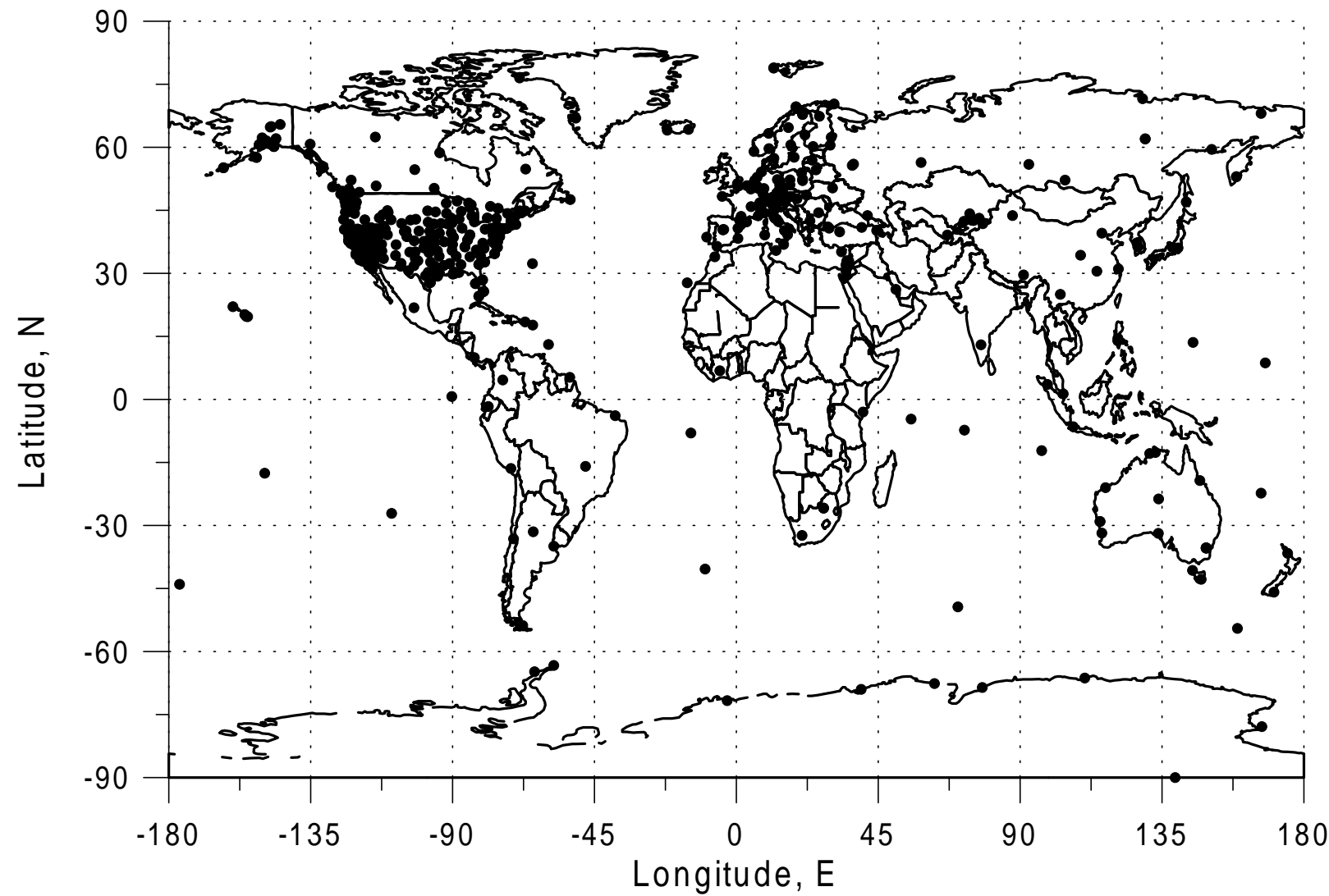
[49] Schaer, S., Gurtner, W. and Feltens, J., IONEX: The IONosphere Map EXchange Format Version 1. Proceeding of the IGS AC Workshop, Darmstadt, Germany, February 9-11; Editor J.W.Dow, 233–247, 1998.

- [50] Shan, S.J., Lin, J.Y., Kuo, F.S. et al. GPS phase fluctuation observed along the American sector during low irregularity activity months of 1997-2000. *Earth, Planets and Space*, 54(2), 141–152, 2002.
- [51] Skone, S., and M. de Jong, The impact of geomagnetic substorms on GPS receiver performance. *Earth, Planets and Space*, 52, 1067–1071, 2000.
- [52] Skone, S. and M. de Jong, Limitations in GPS receiver tracking performance under ionospheric scintillation. *Physics and Chemistry of the Earth, Part A*, 26/6-8, 613–621, 2001.
- [53] Spoelstra, T. A., Kelder, H., Effects produced by the ionosphere on radio interferometry. *Radio Sci.*, 19, pp. 779–788, 1984.
- [54] Thompson, R., Moran, J. and Swenson, Dj. *Interferometry and Synthesis in Radio Astronomy*. John Wiley and Sons, Inc., 1986.
- [55] Warnart, R. The study of the TEC and its irregularities using a regional network of GPS stations. *IGS worksh. Proc.* 249–263, 1995.
- [56] Wilson, B. D., Mannucci, A. J. and Edwards, C. D., Subdaily northern hemisphere maps using the IGS GPS network. *Radio Sci.*, 30, 639–648, 1995.
- [57] Yakovlev, O. I. *The Propagation of Radio Waves in Space*. Moscow: Nauka, 1985, p. 214.
- [58] Yakubov, V. P. *Doppler Very-Long-Baseline Interferometry*. Tomsk: Vodolei, 1997, p. 246.

Table 1: Statistics of experiments for mid-latitudes

N	Date	Day number	m	n	$\langle P \rangle$ %	P_{max} , %	Dst_{max} , nT	Kp_{max}
1	29.07.1999	210	160	1653	0.017	0.17	-40	3
2	9.01.2000	009	323	4330	0.06	0.27	-13	—
3	6.04.2000	097	243	1949	0.67	2.4	-293	8
4	15.07.2000	197	306	4114	0.34	4	-295	9

GPS global network



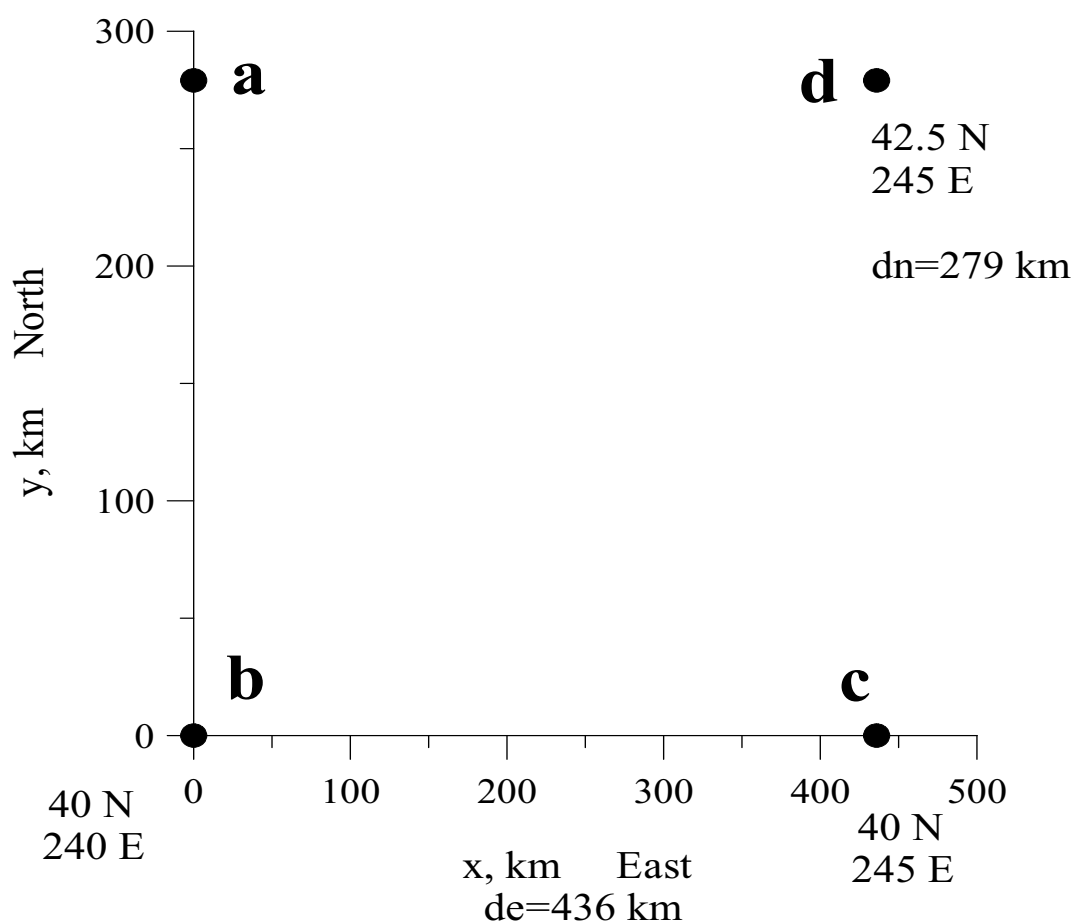


Figure 2: Geometry of an elementary GIM cell. Nodes of the cell are denoted *a*, *b*, *c*, and *d*. The cell size is determined by the values of $d_n = 279$ km and of d_e dependent on the cell's location latitude.

This figure "Fig3asl.jpg" is available in "jpg" format from:

<http://arxiv.org/ps/physics/0212046v2>

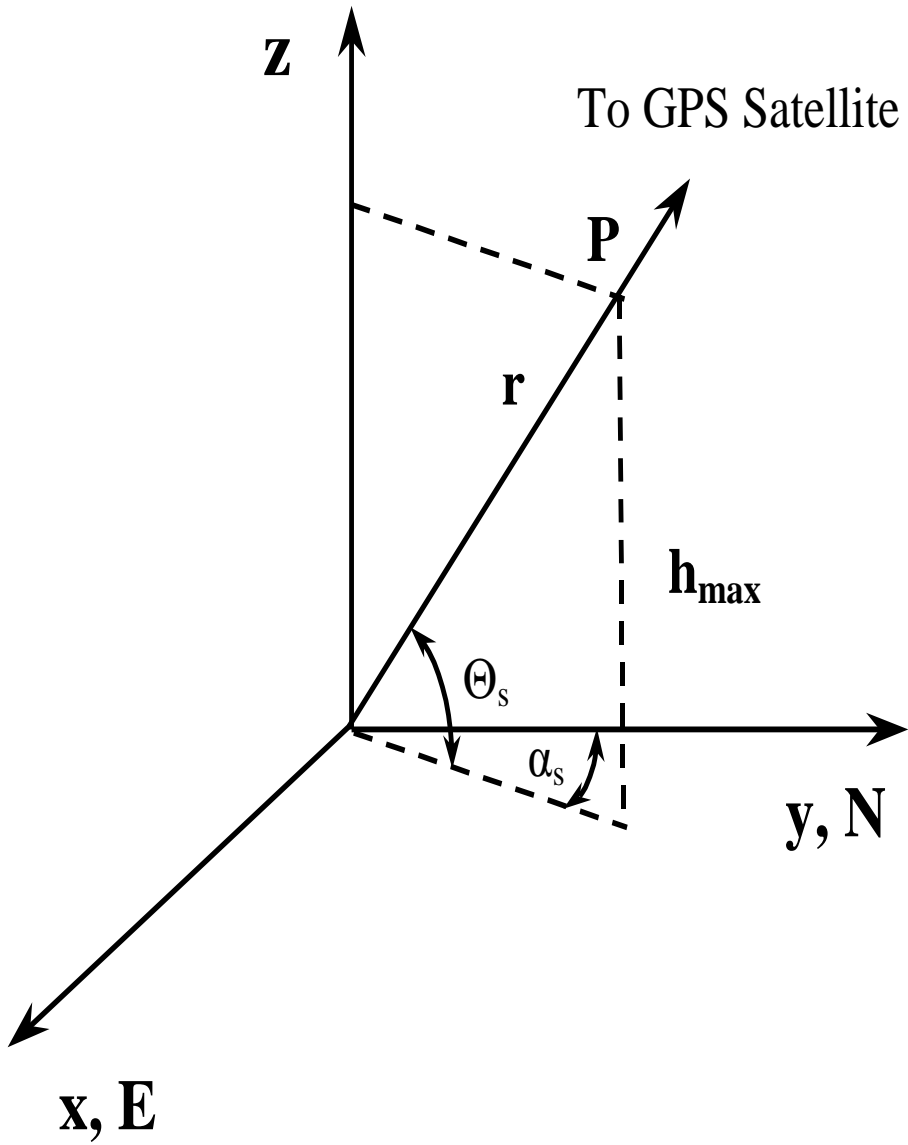
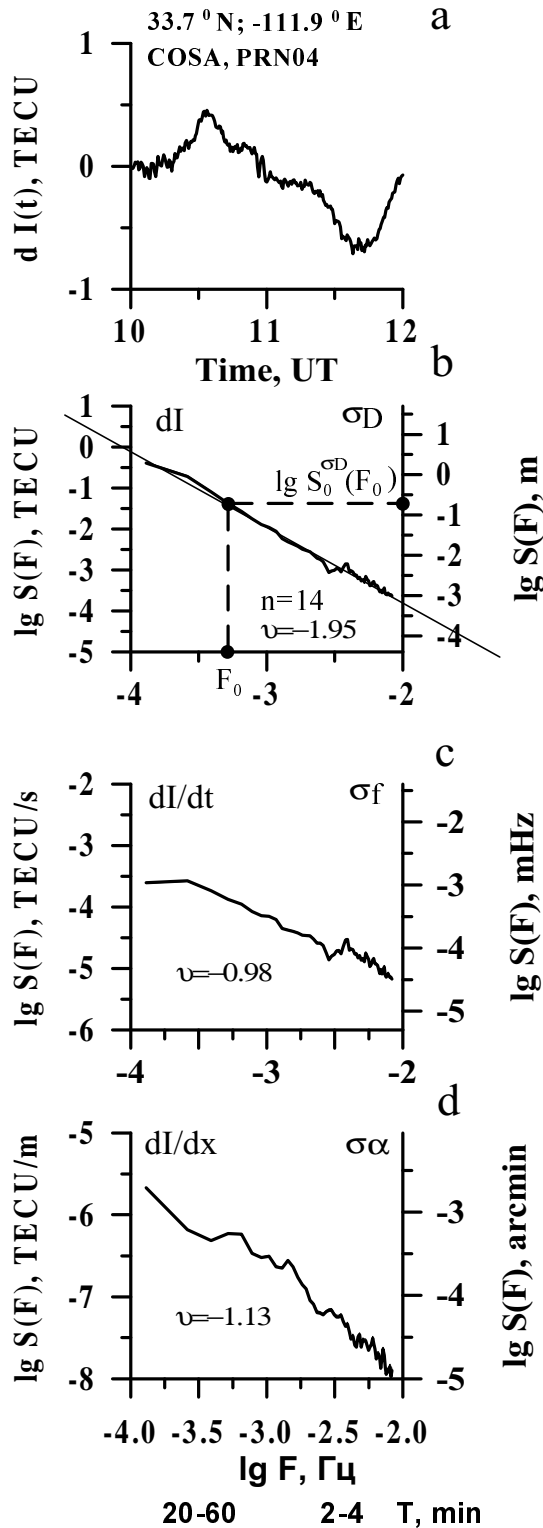
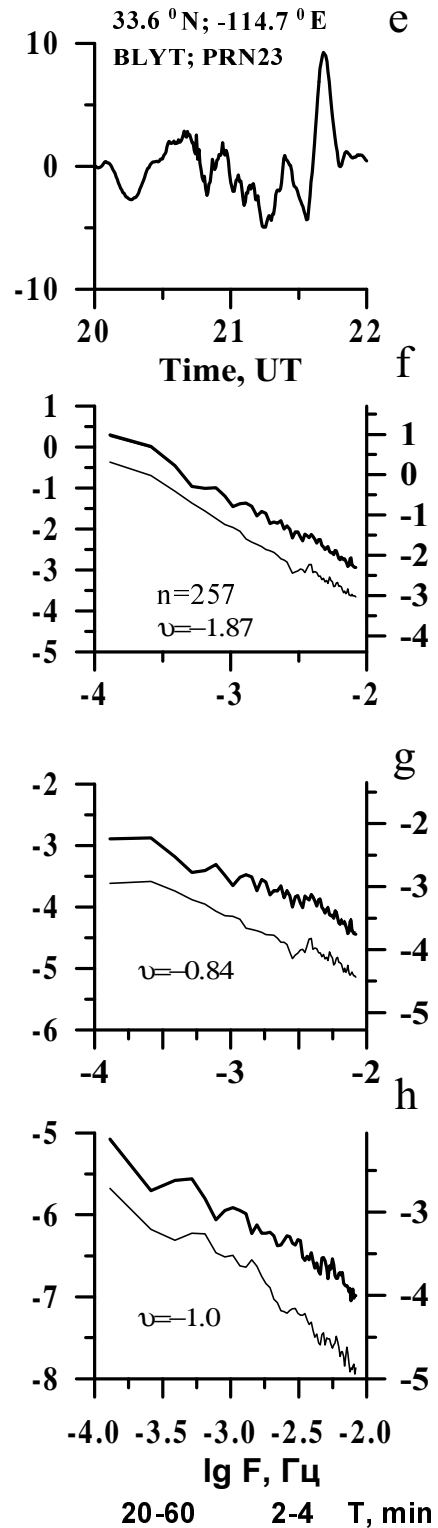


Figure 4: Schematic representation of the transitionospheric sounding geometry. The axes z , y and x are directed, respectively, zenithward, northward (N) and eastward (E). P – point of intersection of Line-of-Sight (LOS) to the satellite with a horizontal plane at the height of the maximum of the ionospheric F_2 – region h_{max} ; S – subionospheric point; and Θ_s , α_s – azimuth and elevation of the direction \mathbf{r} along LOS to the satellite.

July 29, 1999



July 15, 2000



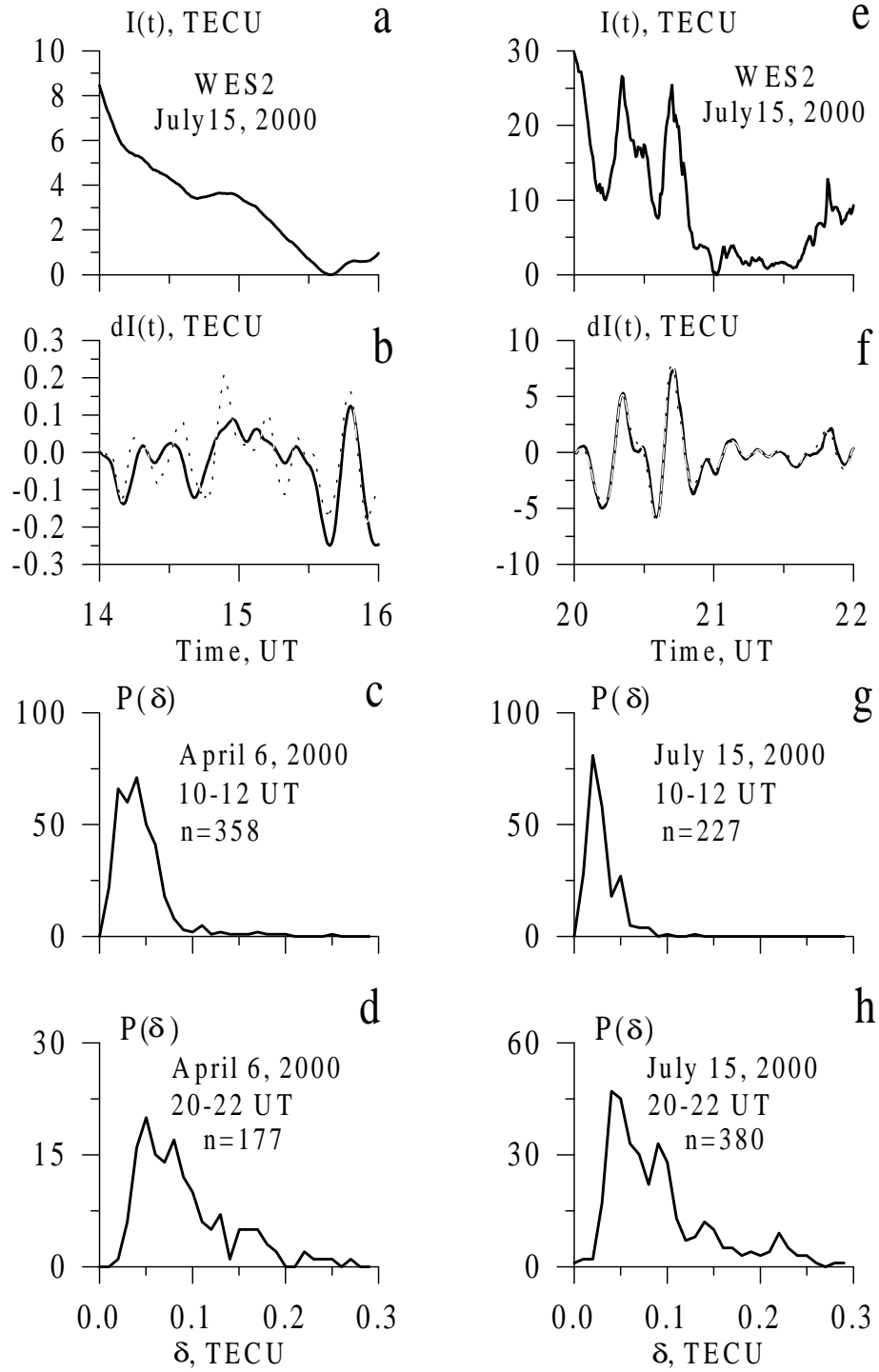
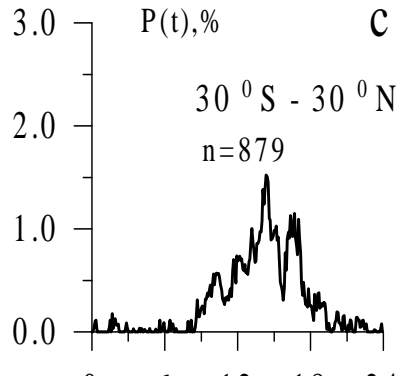
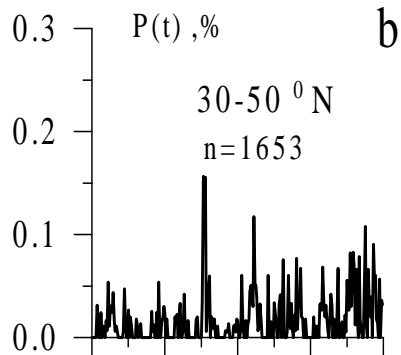
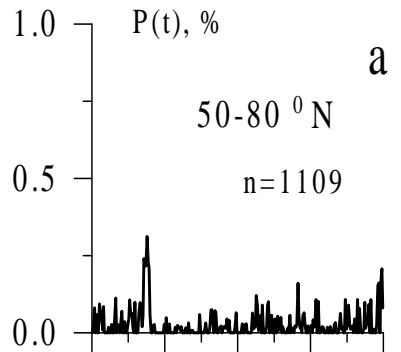


Figure 6: Time dependencies of the "vertical" TEC $I(t)$, measured at station WES2 – a) prior to the onset of the geomagnetic disturbance of July 15, 2000, and at station WES2 thereafter – e). The $dI(t)$ variations filtered from the $I(t)$ series by removing the trend with a 60-min window for this stations – b); f). For comparison, the dashed line in panels b and f plots the $dI(t)$ variations calculated from values of the pseudo-range $C1$ and of the phase $L1$. Distributions $P(\delta)$ of the standard deviation δ of the TEC variations obtained in phase measurements at two frequencies $L1 - L2$ and at the $L1$ only – c, d, g, h.

July 29,1999

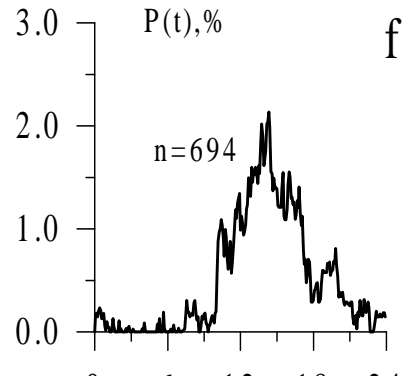
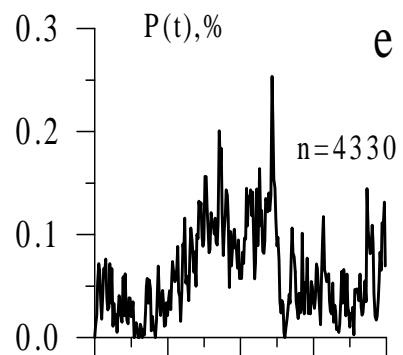
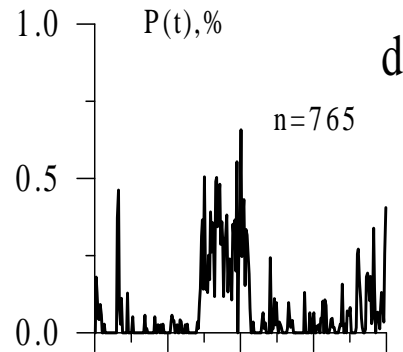
0-360°E



Time, LT

January 9, 2000

0-360°E



Time, LT

Figure 7: Local time LT-dependence of the relative mean slip density $P(t)$, obtained by averaging the data from all GPS satellites in the longitude range $0 - 360^\circ$ E irrespective of the type of GPS receivers for the magnetically quiet days of July 29, 1999 (at the left), and January 9, 2000 (at the right): a, d – high latitudes $50 - 80^\circ$ N; b, e – mid-latitudes $30 - 50^\circ$ N; and c, f – equatorial zone 30° S- 30° N.

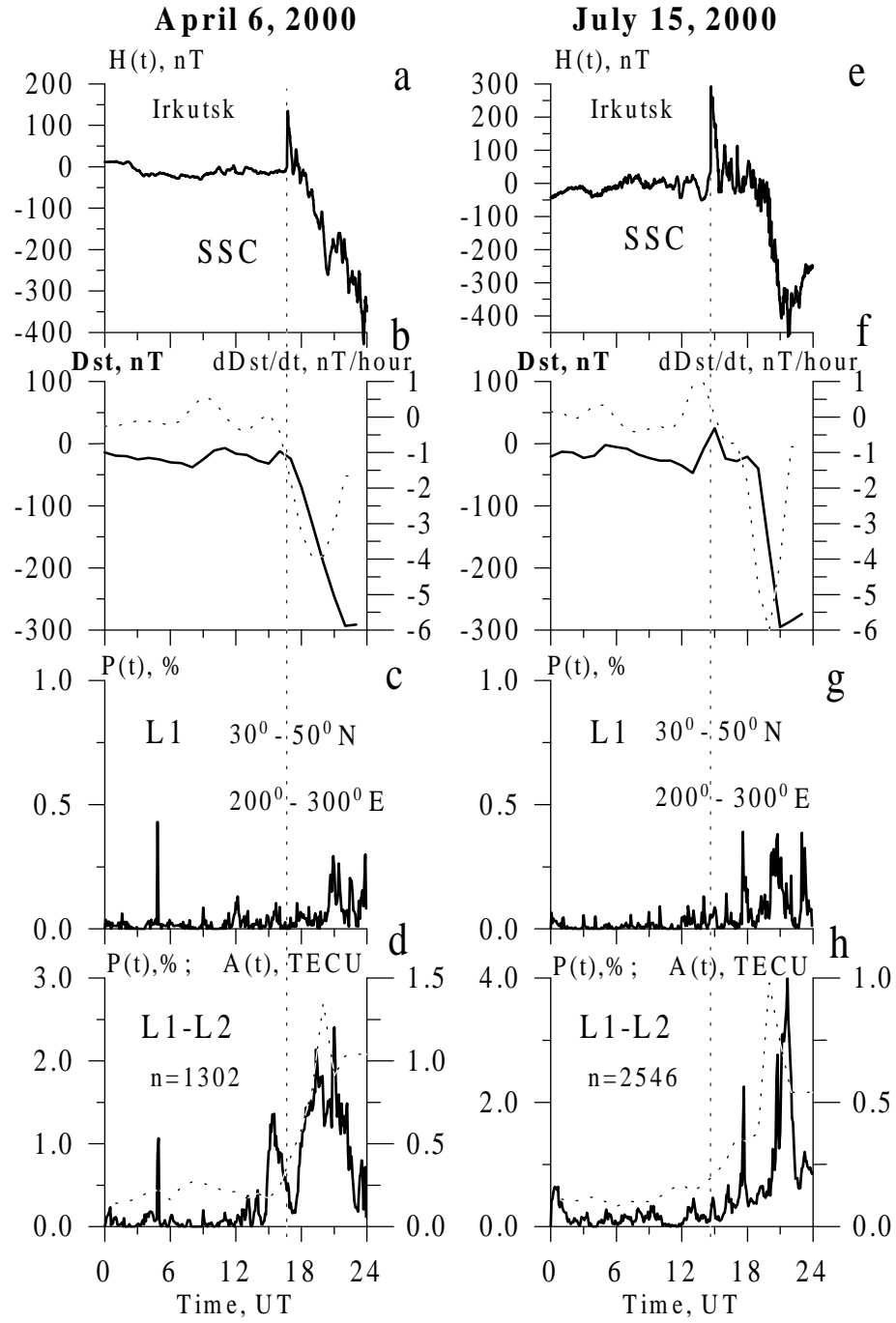
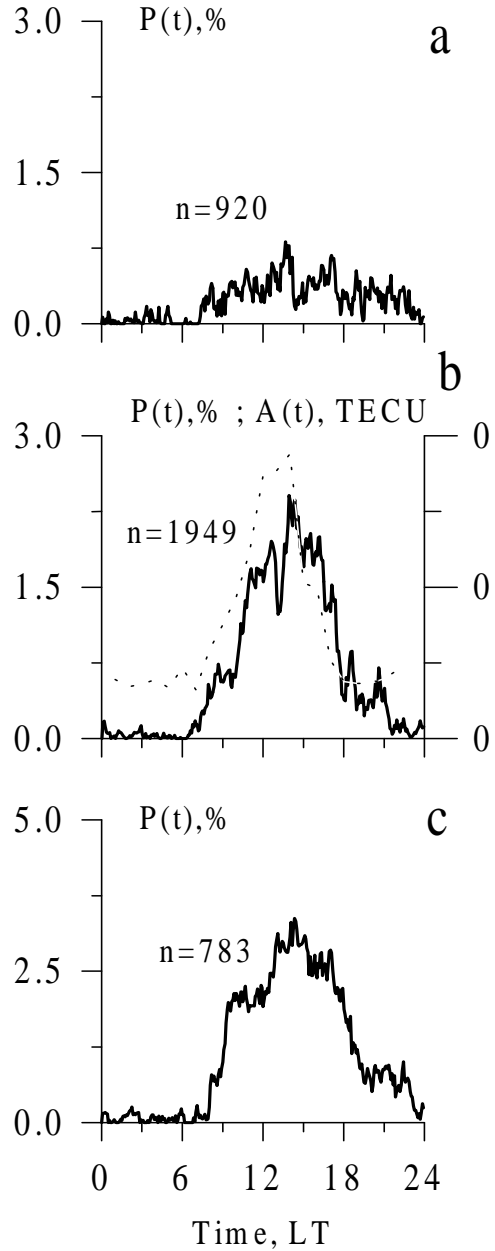


Figure 8: Variations of the H -component of the geomagnetic field record at station Irkutsk – a), Dst – b), thick line, and the dependence of the time derivative $d(Dst(t))/dt$ – b), dashed line, during the magnetic storm of April 6, 2000. The UT-dependence of the relative mean $L1 - L2$ slip density $P(t)$ – d), thick line. For comparison, the panel c) plots the relative mean $L1$ slip density $P(t)$. The same dependencies for a magnetic storm of July 15, 2000 - e, f, g, h. The SSC times 16:42 UT and 14:37 UT are shown by a vertical bar. For comparison, the dashed line in panels d and h plots the dependencies $A(t)$ of the TEC variation intensity obtained for the same set of stations as in the case of $P(t)$.

April 6, 2000

30 - 50⁰ N ; 0 - 360⁰ E



July 15, 2000

30 - 50⁰ N ; 0 - 360⁰ E

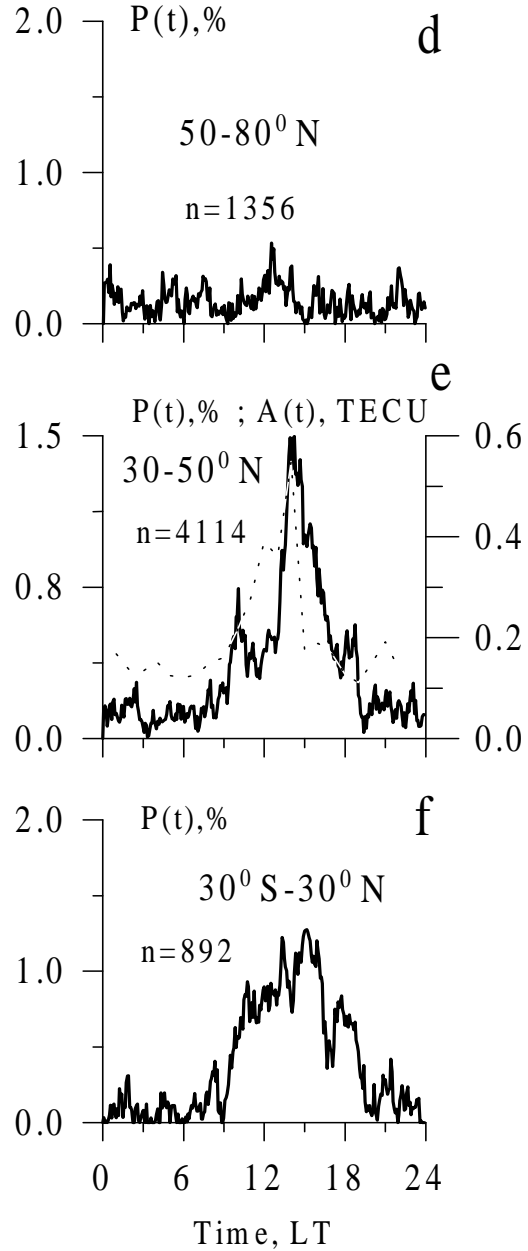


Figure 9: Same as in Figure 3, but for the magnetic storms on April 6 (at the left) and July 15, 2000 (at the right) at mid latitudes. For comparison, the dashed line in panels b and e plots the dependencies $A(t)$ of the TEC variation intensity obtained for the same set of stations as in the case of $P(t)$.

April 6, 2000
30-50⁰ N; 200-300⁰ E

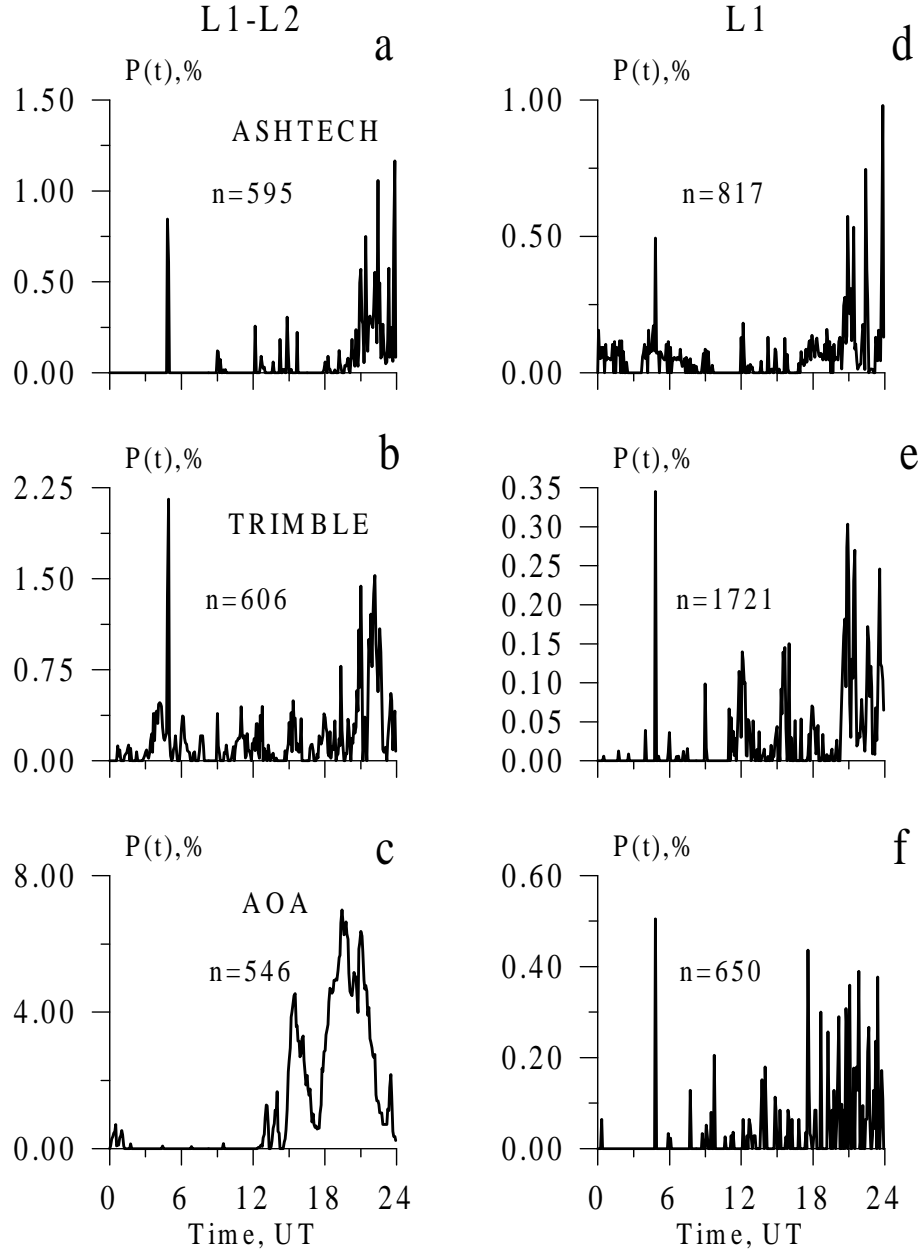


Figure 10: UT-dependencies of the relative mean slip density $P(t)$ of $L1 - L2$ phase measurements (at the left) and phase measurements of $L1$ only (at the right) for a major magnetic storm of April 6, 2000 (ASHTECH – a, d, TRIMBLE – b, e, and c, f – AOA receivers).

April 6, 2000

30° S - 30° N; 0° - 360° E

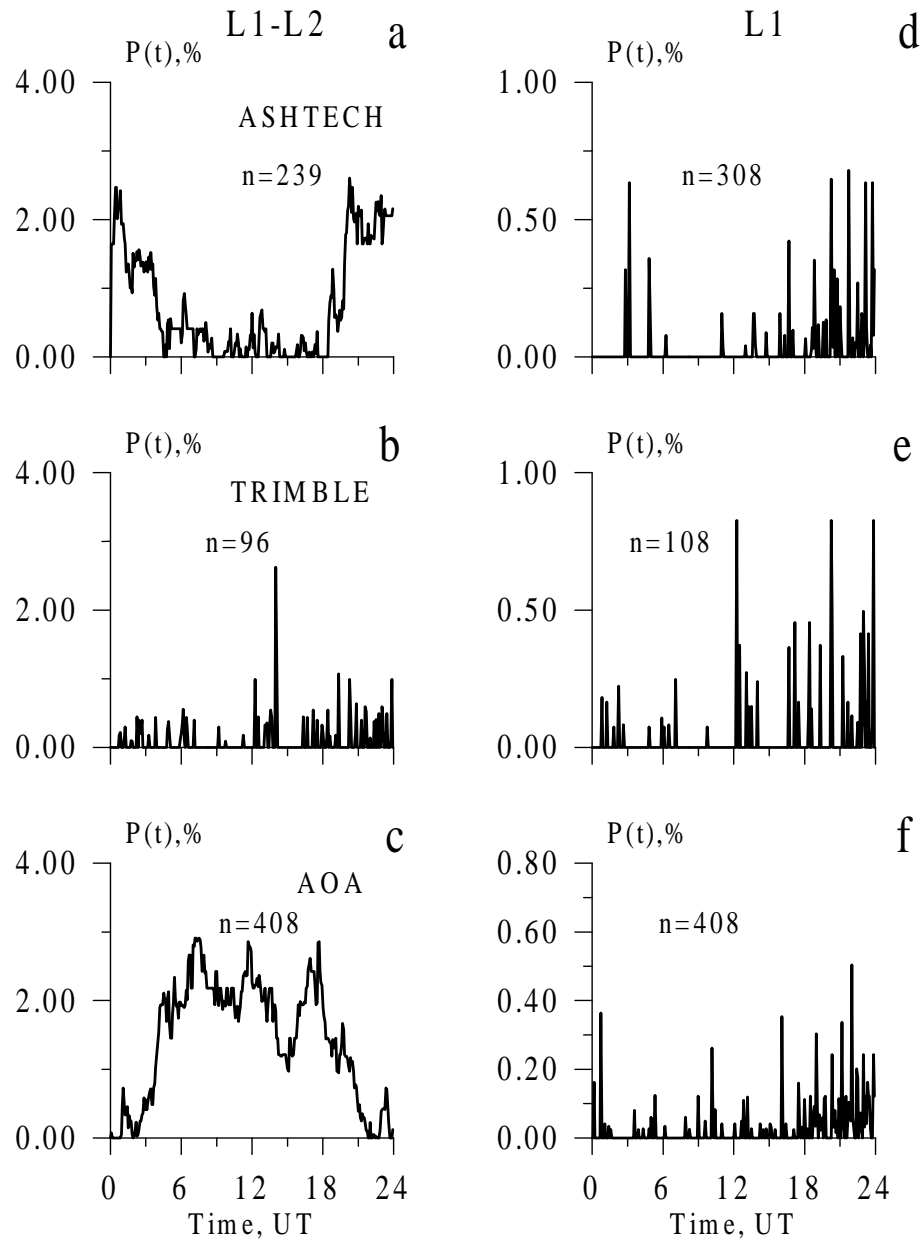


Figure 11: Same as in Figure 10, but at the equatorial zone 30° S- 30° N.